Title: Photons from the Edge: Revealing Black Holes with the Event Horizon Telescope

Date: Jun 23, 2015 02:00 PM

URL: http://pirsa.org/15060021

Abstract: The Event Horizon Telescope, global array of millimetre telescopes, has now enabled studies of nearby supermassive black holes on sub-horizon length scales. This unprecedented access opens a window onto not only the high-energy astrophysics of black hole accretion and jet formation, but also the nature of gravity in the heretofore unexplored strongly non-linear regime near the black hole horizon. I will summarize the state of the Event Horizon Telescope, what results obtained over the past 7 years, and how a revolution in capability will produce precision tests of strong gravity over the next 2-3 years.

ASTRONOMY: ACTIVE DRIVERS VS. PASSIVE ACTORS

$L \sim 10^{47}$ erg/s

ASTRONOMY:
ACTIVE DRIVERS VS. PASSIVE ACTORS

$L \sim 10^{48}$ erg/s

10^{13} Suns

1 SNe/15 min

(cf. 1 SNe/Century in MW!)

Outshines galaxy 100x !

ASTRONOMY:
ACTIVE DRIVERS VS. PASSIVE ACTORS

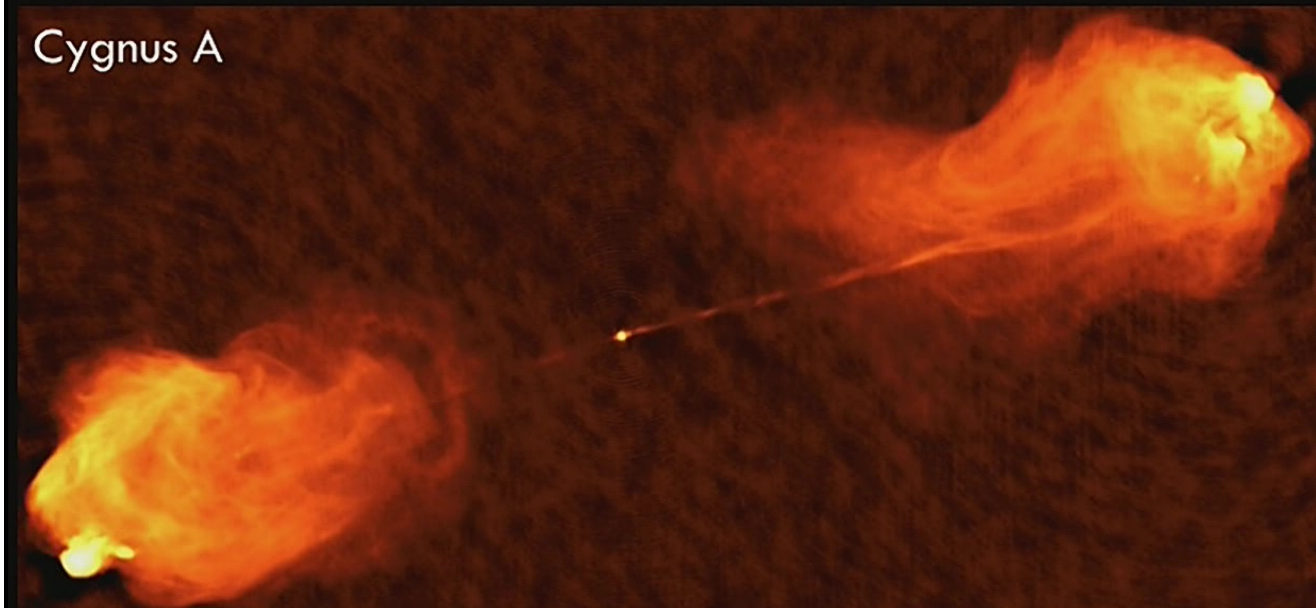

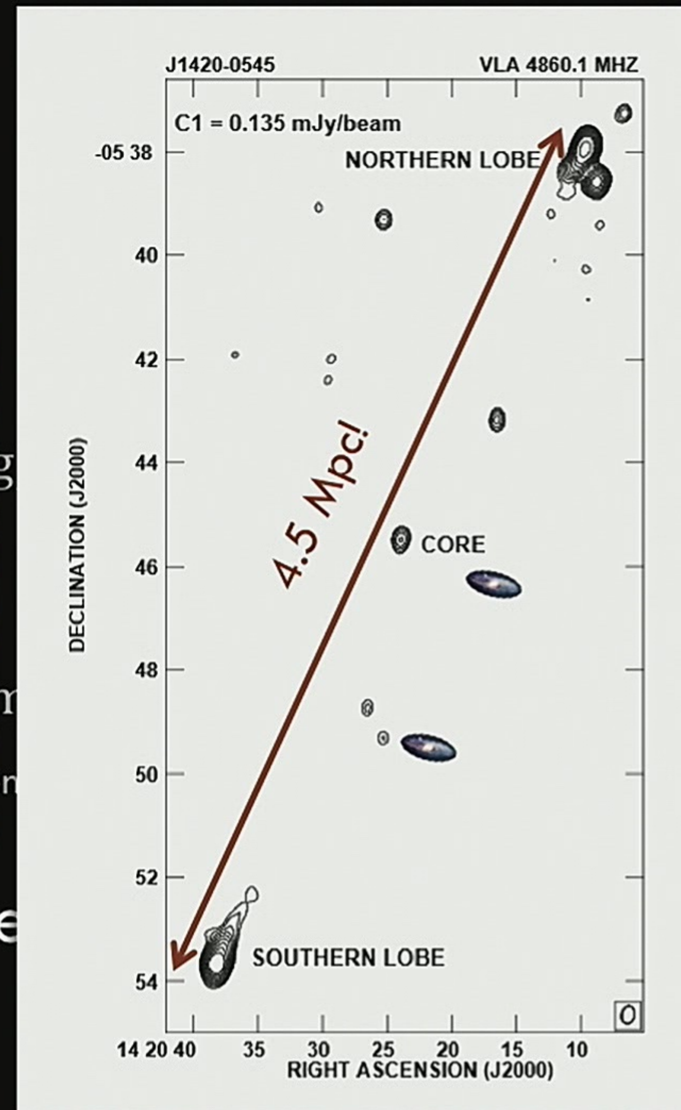

Outshine

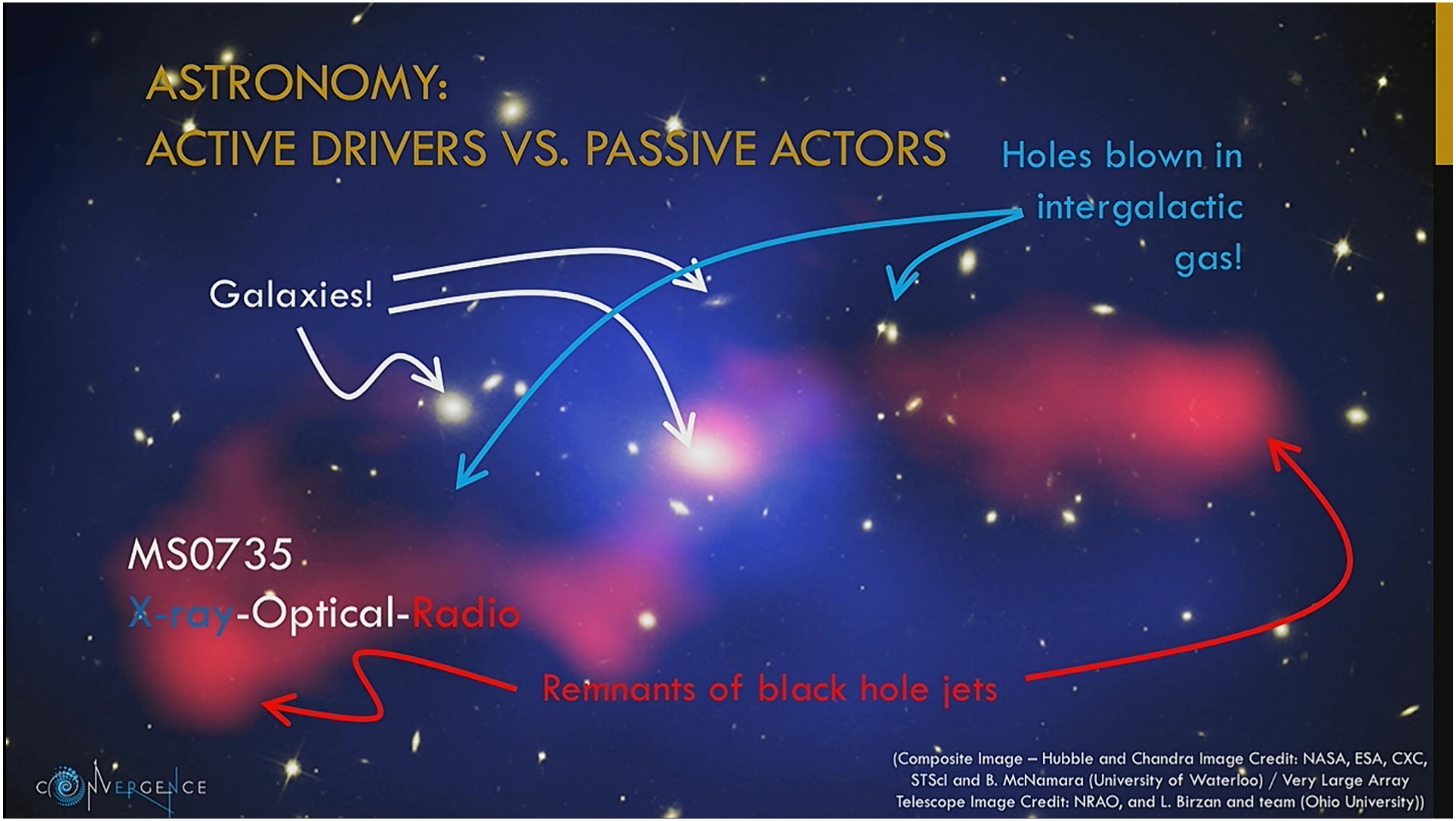
ASTRONOMY:
ACTIVE DRIVERS VS. PASSIVE ACTORS
Holes blown in intergalactic gas!
Galaxies!
MS0735
X-ray-Optical-Radio
Remnants of black hole jets
(Composite Image – Hubble and Chandra Image Credit: NASA, ESA, CXC, STScI and B. McNamara (University of Waterloo) / Very Large Array Telescope Image Credit: NRAO, and L. Birzan and team (Ohio University))
CONVERGENCE

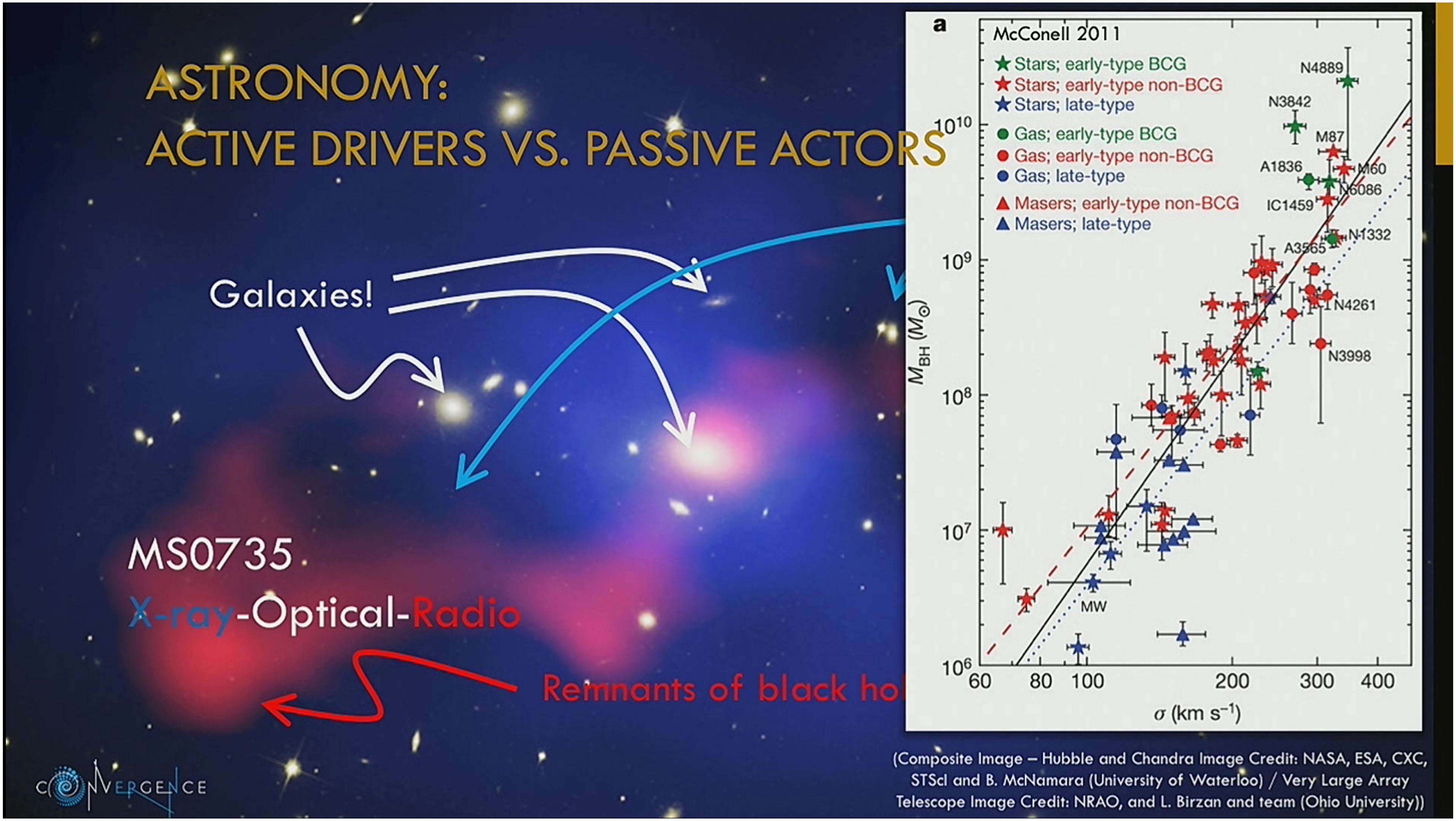
ASTRONOMY:
ACTIVE DRIVERS VS. PASSIVE ACTORS
Galaxies!
MS0735
X-ray-Optical-Radio
Remnants of black ho
a
McConell 2011
Stars; early-type BCG
Stars; early-type non-BCG
Stars; late-type
Gas; early-type BCG
Gas; early-type non-BCG
Gas; late-type
Masers; early-type non-BCG
Masers; late-type
N4889
N3842
M87
A1836
M60
N6086
IC1459
N1332
A3565
N4261
N3998
MW
M_{BH} ($M_\odot$)
σ (km s^{-1})
(Composite Image – Hubble and Chandra Image Credit: NASA, ESA, CXC, STScI and B. McNamara (University of Waterloo) / Very Large Array Telescope Image Credit: NRAO, and L. Birzan and team (Ohio University))

PHYSICS:
STRONG GRAVITY

$$\frac{GM}{Rc^2} \sim 1$$

$$\frac{GM}{Rc^2} \sim \frac{G}{Rc^2}\left(\frac{4\pi}{3}\rho R^3\right) \sim 1 \left(\frac{\rho}{1\ \mathrm{H\ atom/m^3}}\right)\left(\frac{R}{10\ \mathrm{Gpc}}\right)^2$$

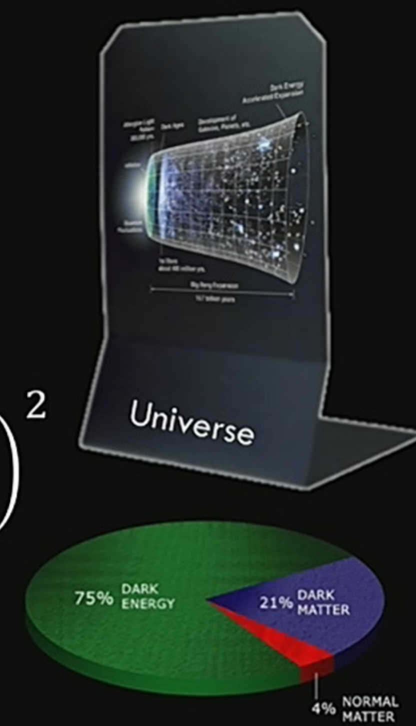

PHYSICS:
STRONG GRAVITY

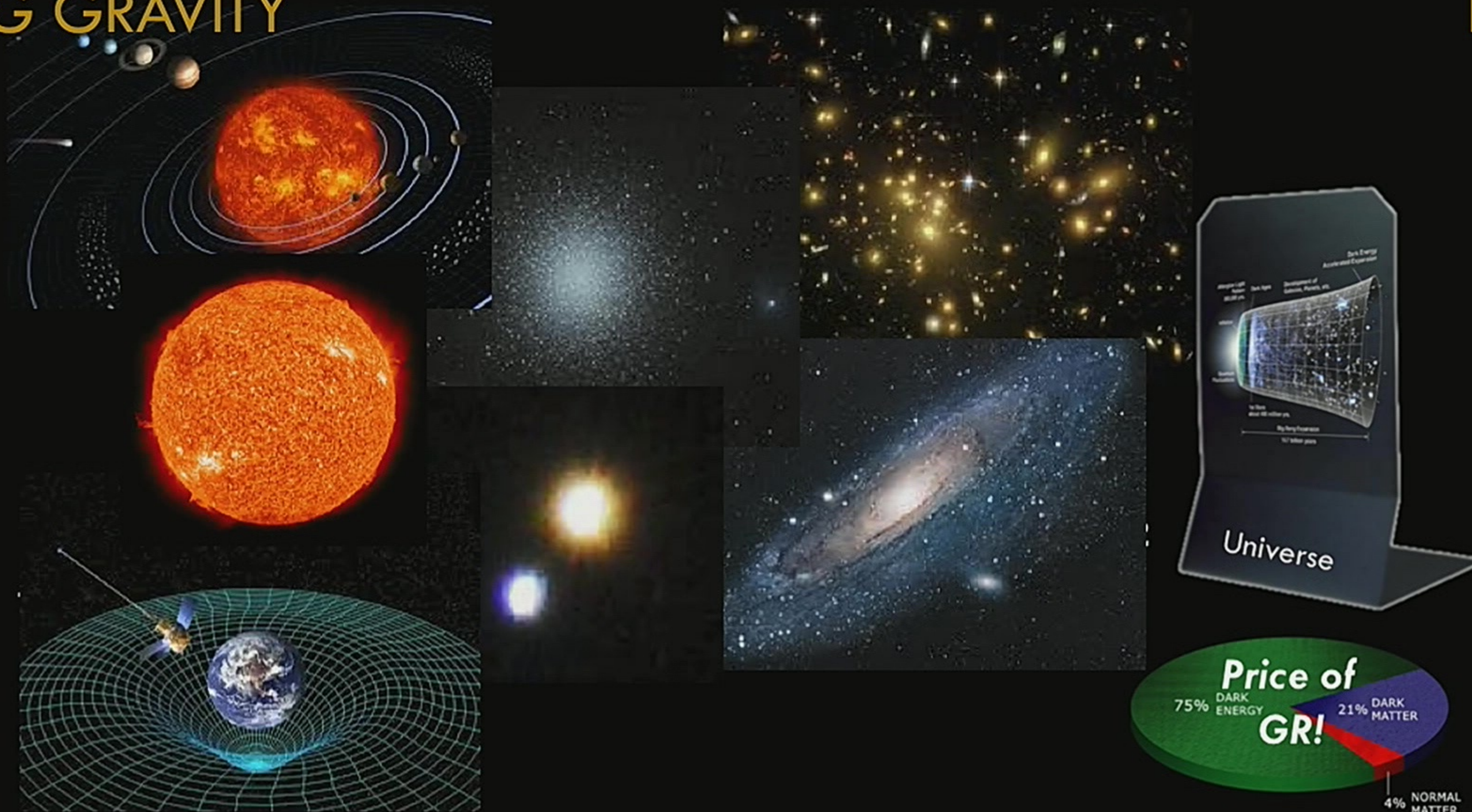

CONVERGENCE

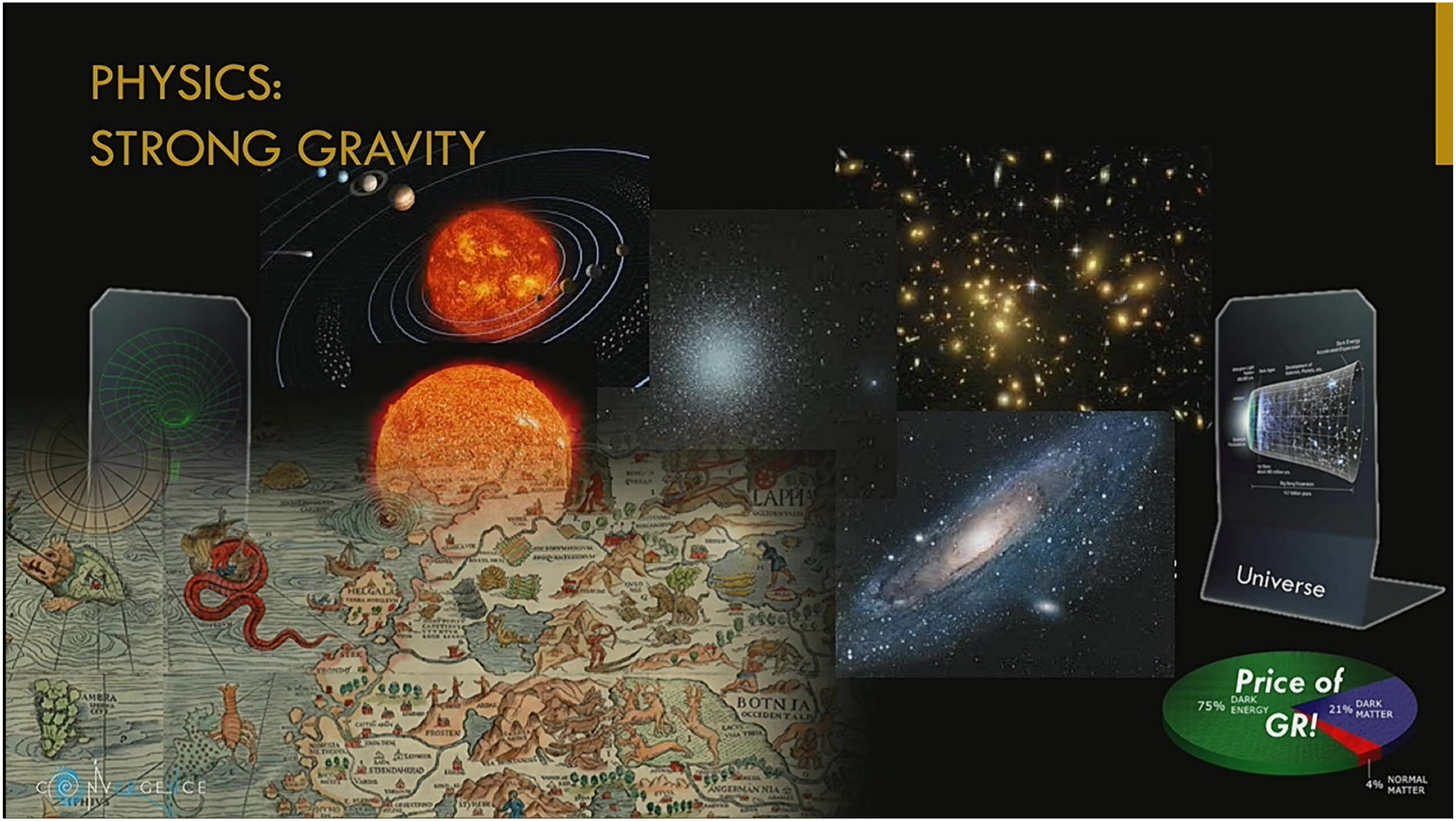
PHYSICS:
STRONG GRAVITY
Universe
Price of GR!
75% DARK ENERGY
21% DARK MATTER
4% NORMAL MATTER
LAPPIA
BOTNIA
HELGALA

"COMPACT" OBJECTS

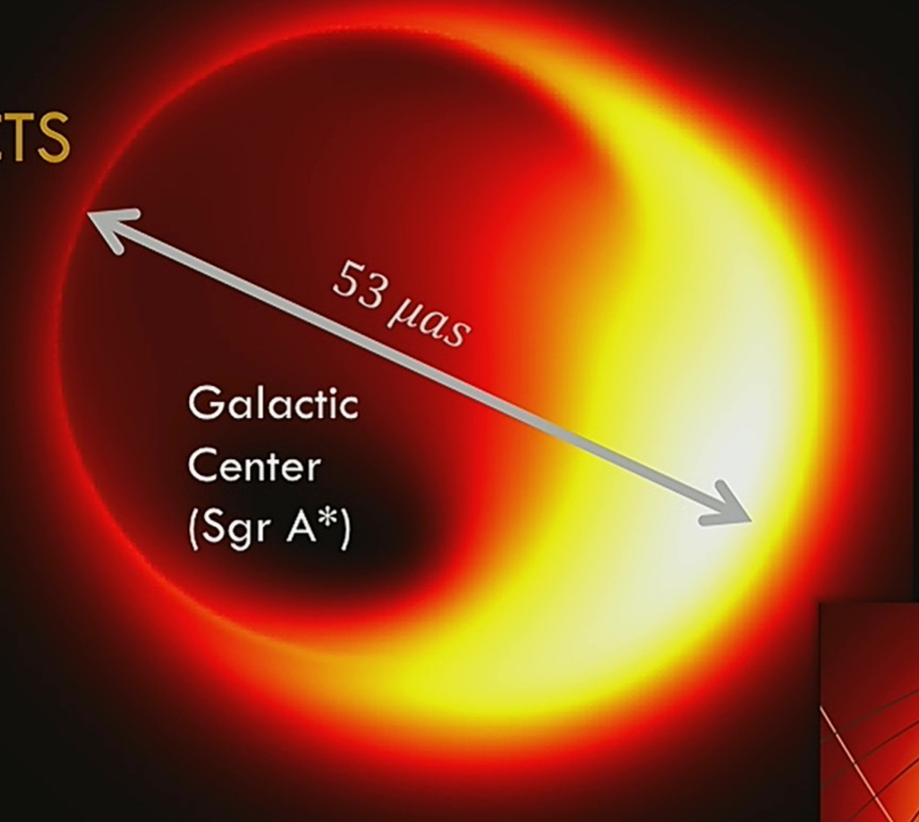

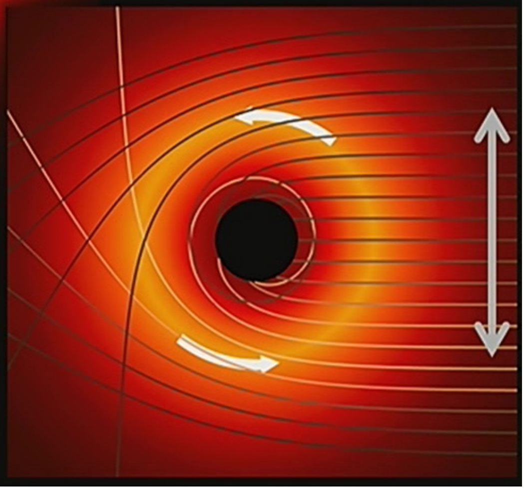

"COMPACT" OBJECTS

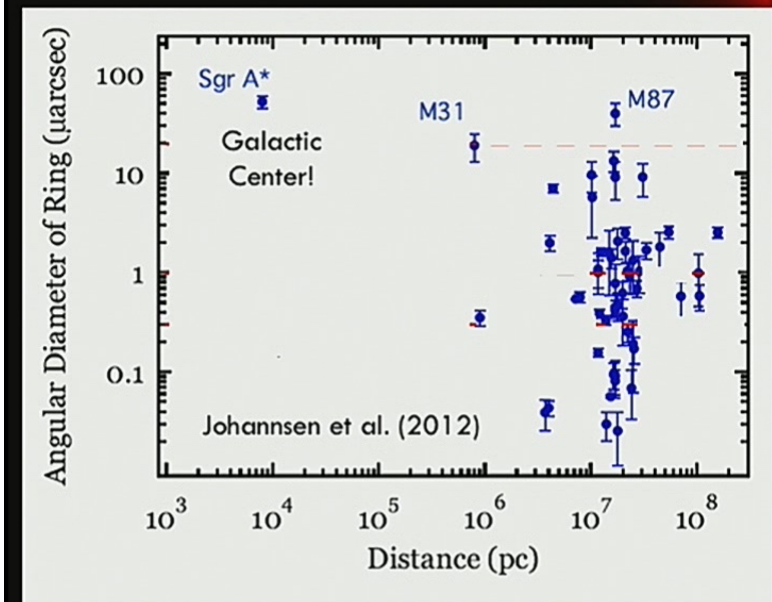

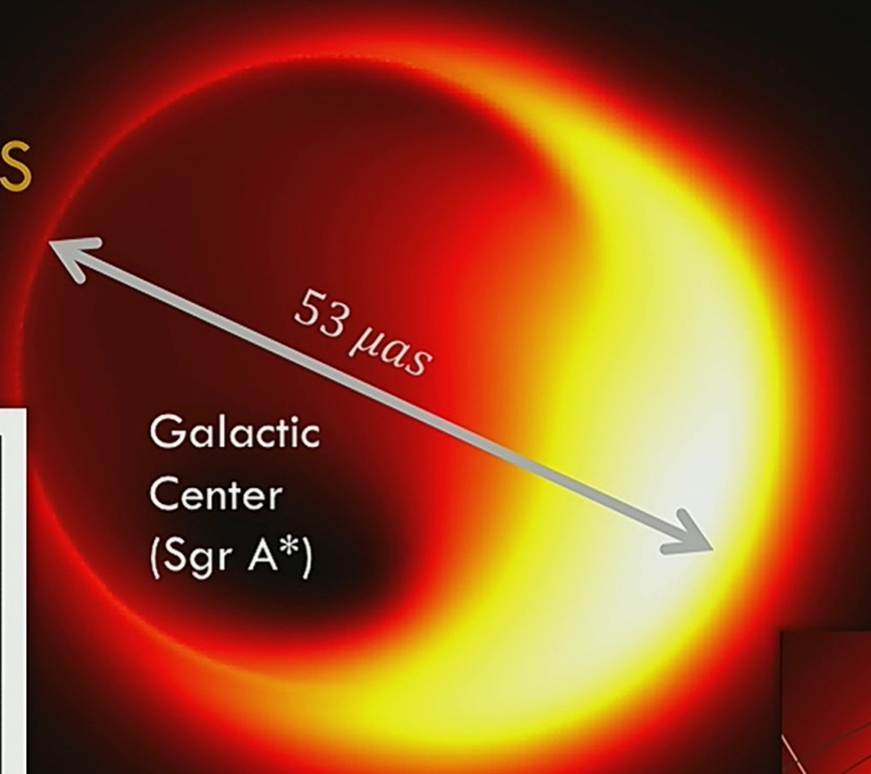

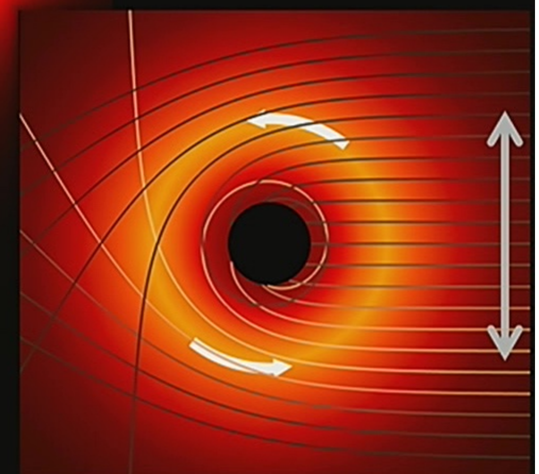

CONVERGENCE

RESOLUTION AND THE DIFFRACTION LIMIT

$$\theta \approx \frac{\lambda}{D}$$

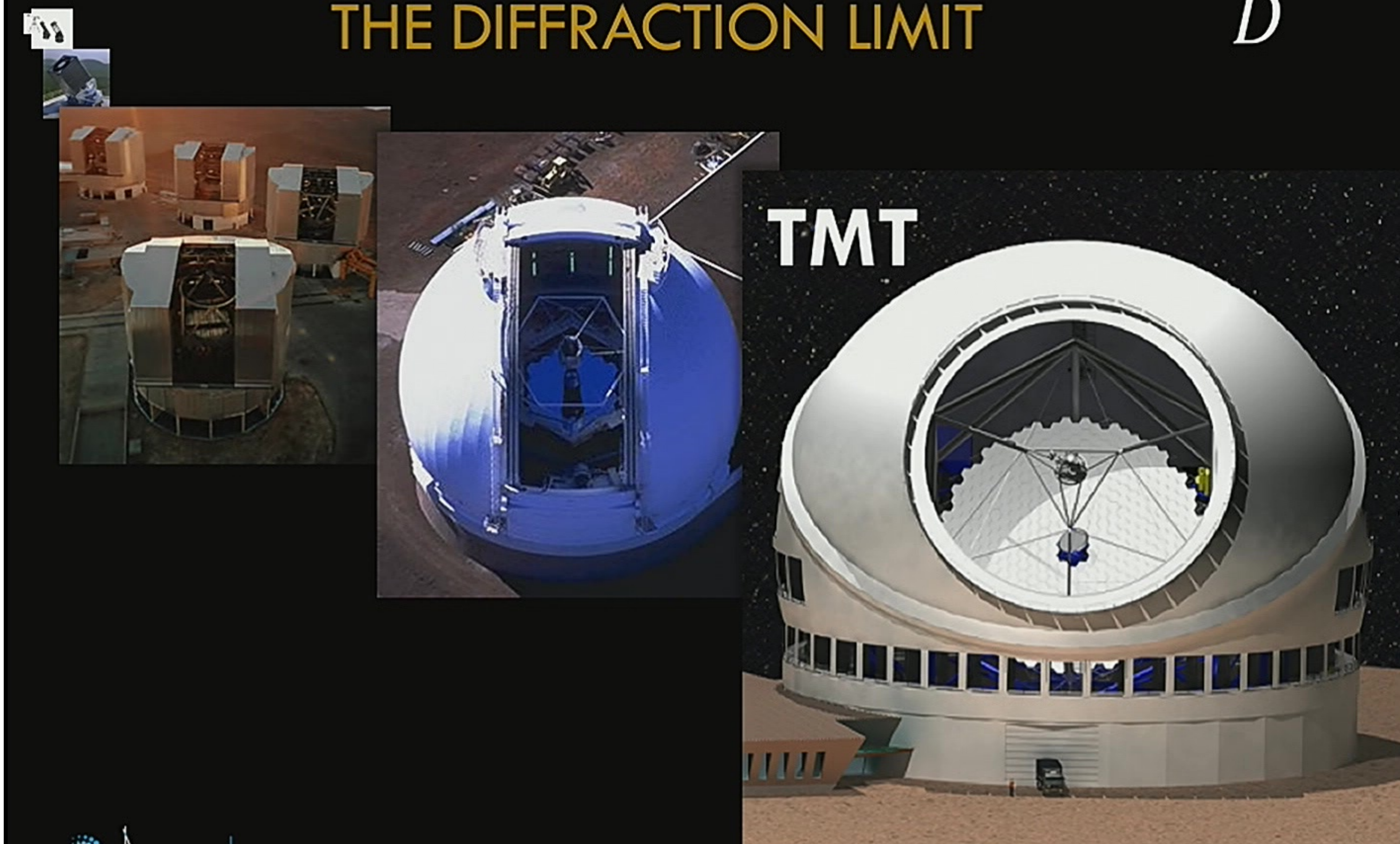

$\theta \sim 7{,}000\ \mu as$

CONVERGENCE

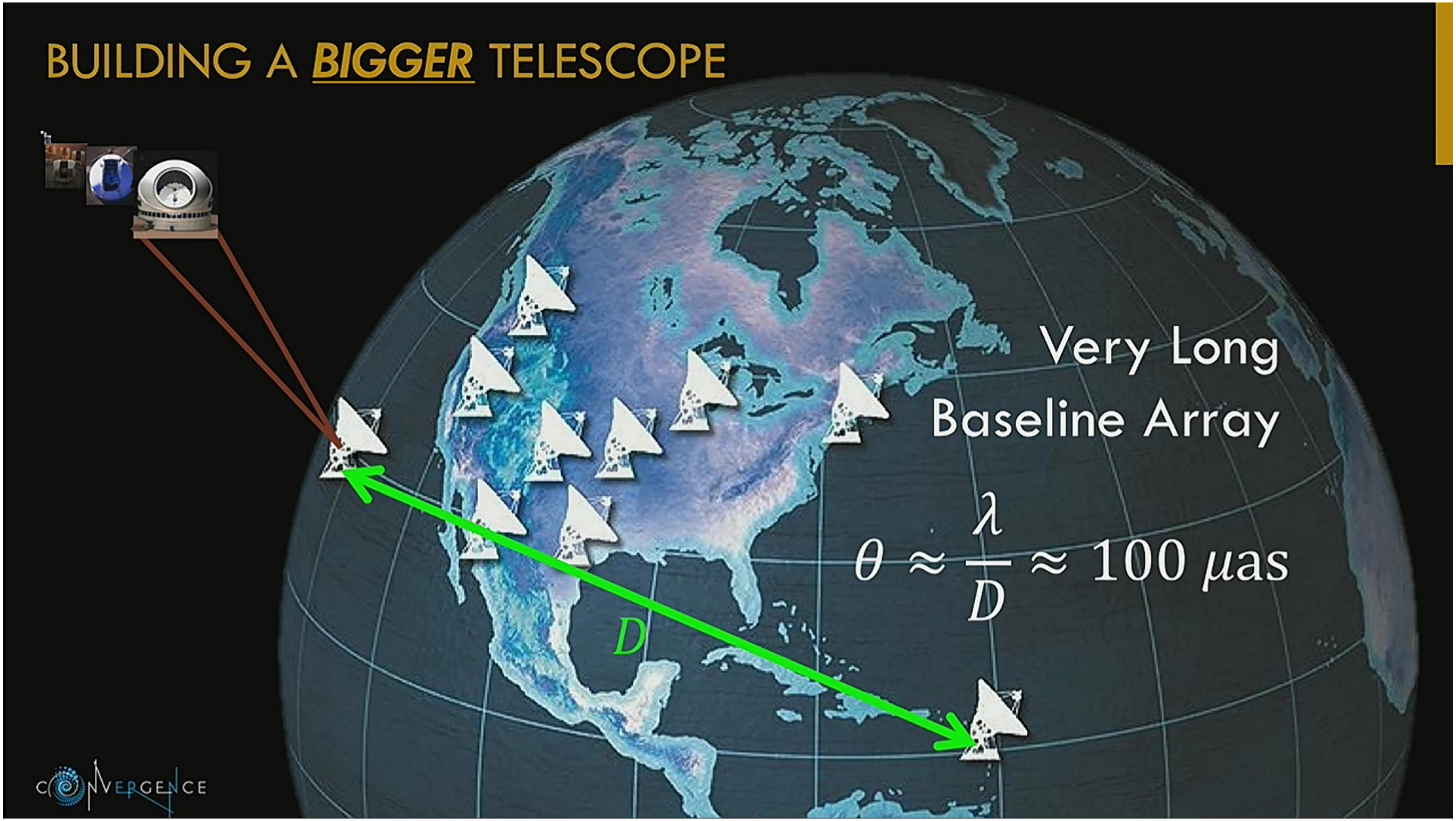
BUILDING A BIGGER TELESCOPE
Very Long
Baseline Array
$\theta \approx \frac{\lambda}{D} \approx 100\ \mu as$
D
CONVERGENCE

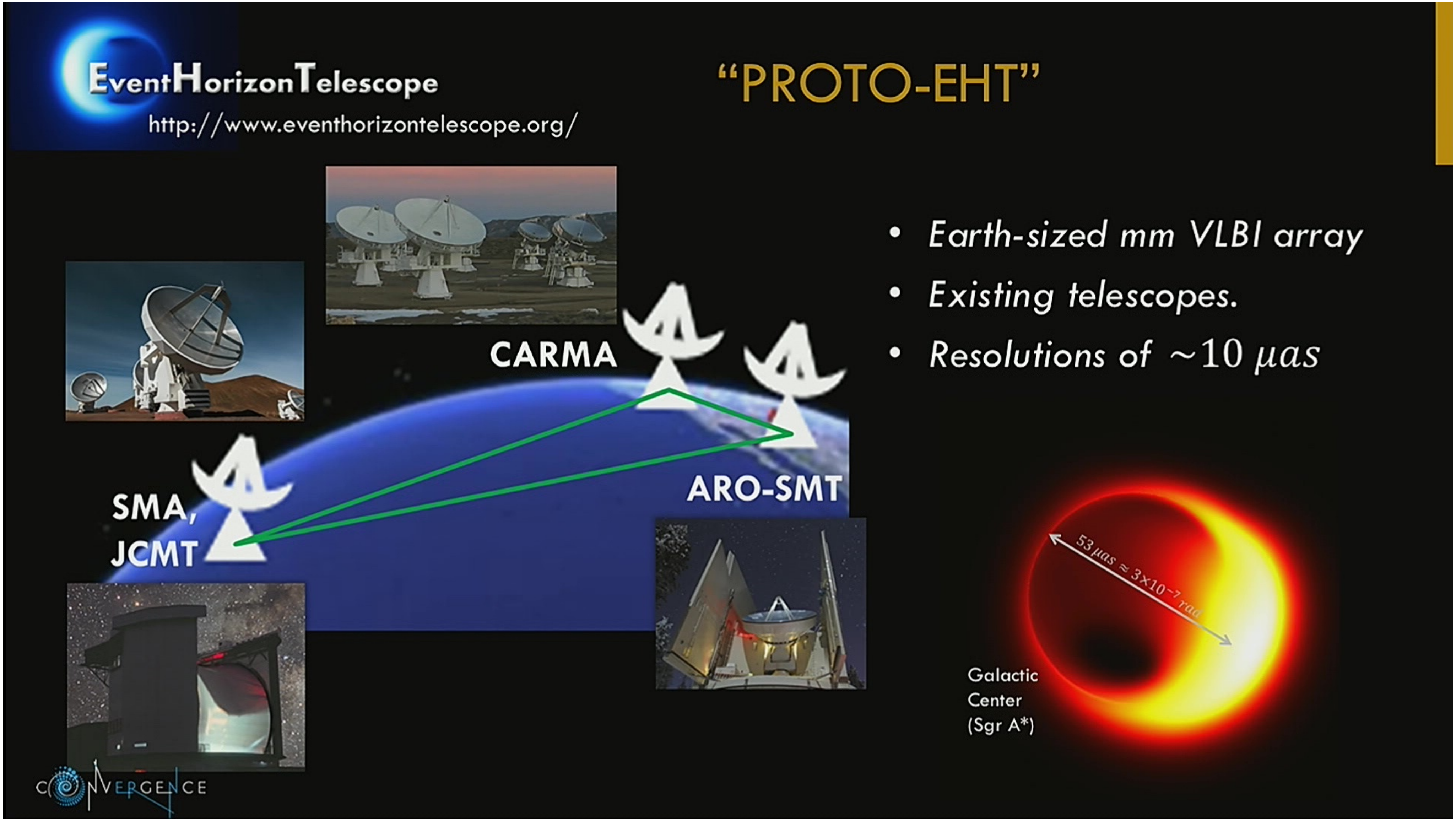
EventHorizonTelescope
http://www.eventhorizontelescope.org/
"PROTO-EHT"
• Earth-sized mm VLBI array
• Existing telescopes.
• Resolutions of ~10 μas
CARMA
SMA,
JCMT
ARO-SMT
53 μas ≈ 3×10⁻⁷ rad
Galactic
Center
(Sgr A*)
CONVERGENCE

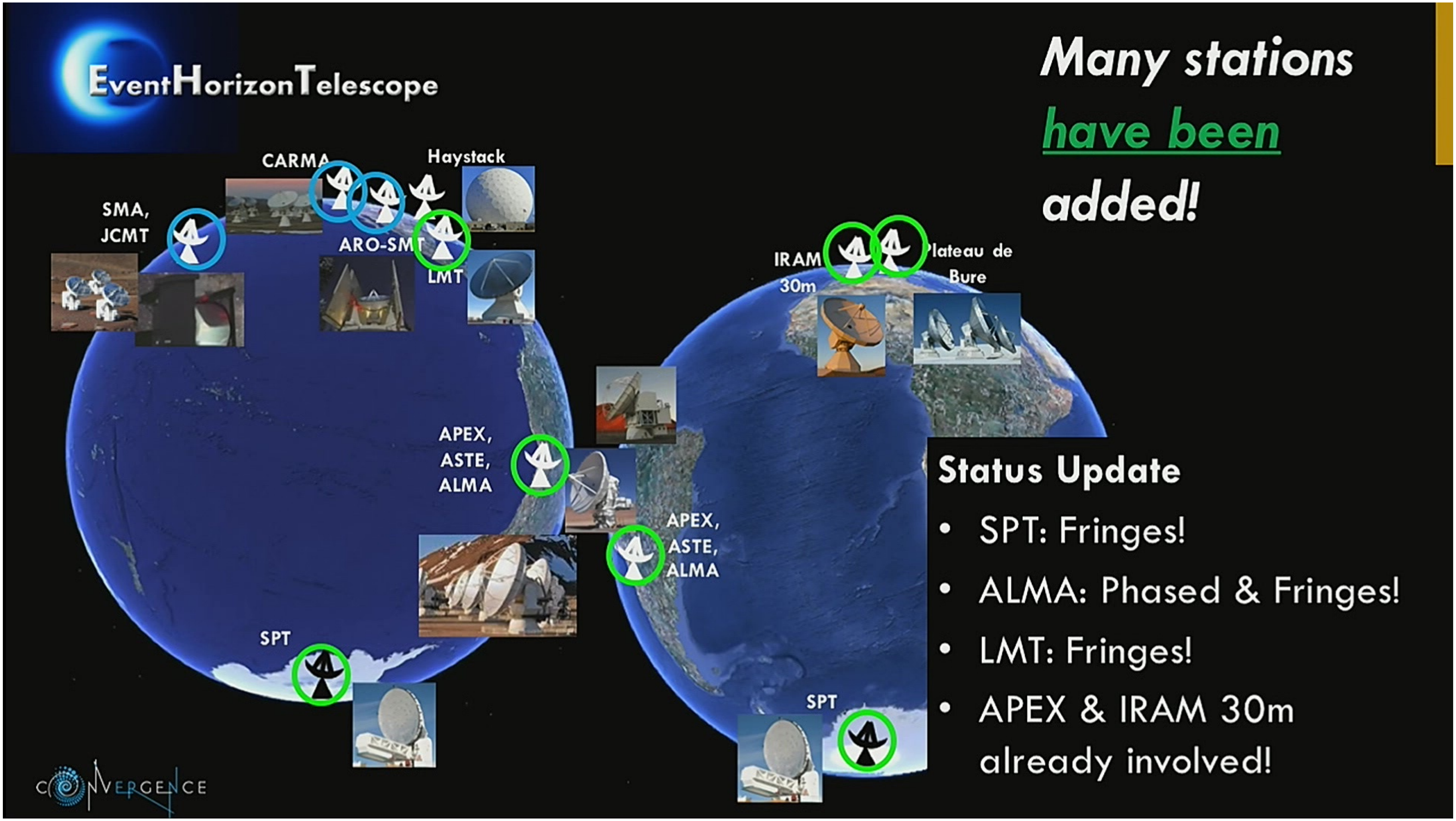
EventHorizonTelescope
Many stations
have been
added!
CARMA
Haystack
SMA,
JCMT
ARO-SMT
LMT
IRAM
30m
Plateau de
Bure
APEX,
ASTE,
ALMA
APEX,
ASTE,
ALMA
SPT
SPT
Status Update
• SPT: Fringes!
• ALMA: Phased & Fringes!
• LMT: Fringes!
• APEX & IRAM 30m already involved!

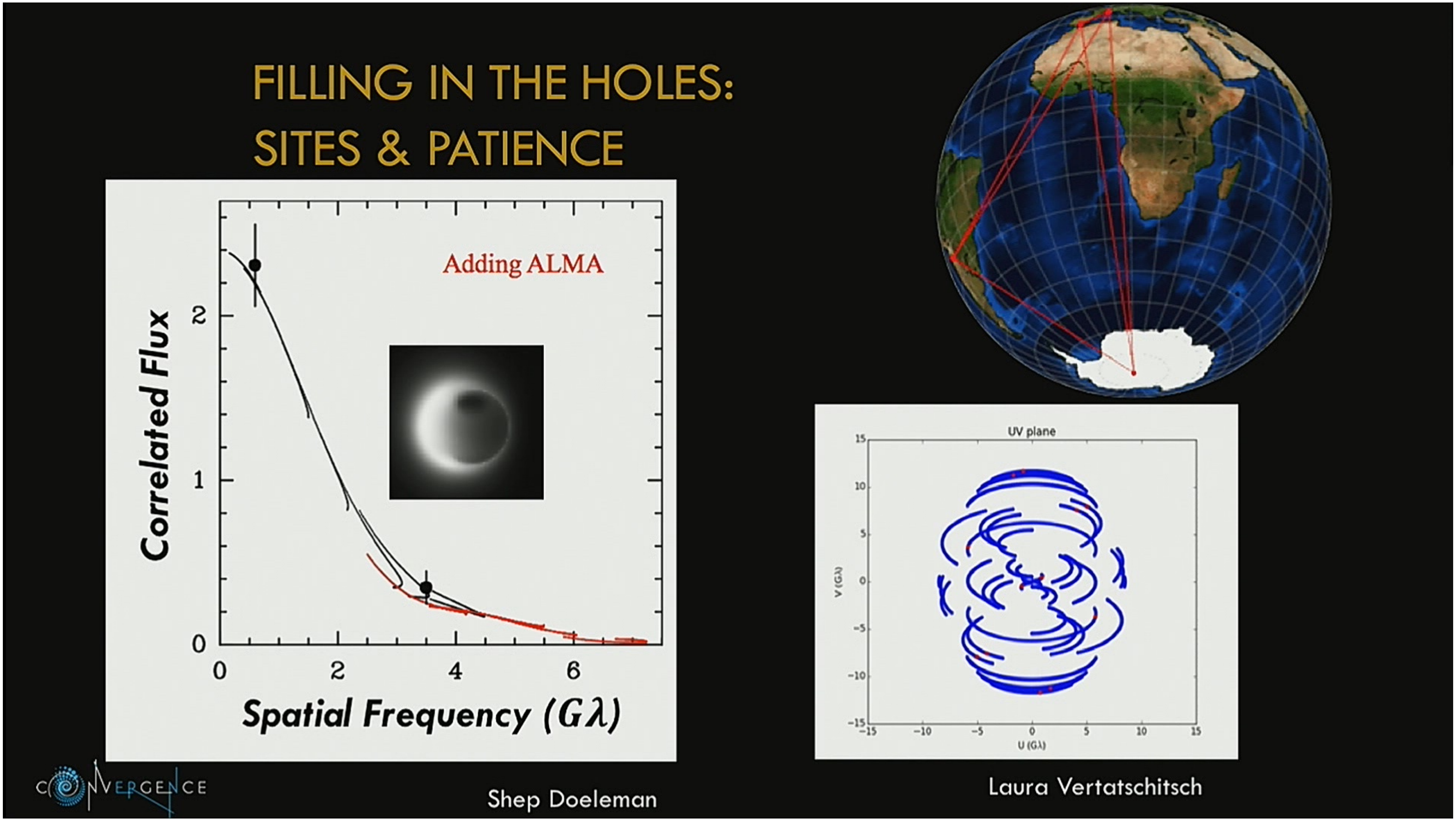
FILLING IN THE HOLES:
SITES & PATIENCE
Adding ALMA
Correlated Flux
Spatial Frequency (Gλ)
0
1
2
0
2
4
6
UV plane
V (Gλ)
U (Gλ)
15
10
5
0
−5
−10
−15
CONVERGENCE
Shep Doeleman
Laura Vertatschitsch

RECONSTRUCTING IMAGES OF SGR A* (DISKS)

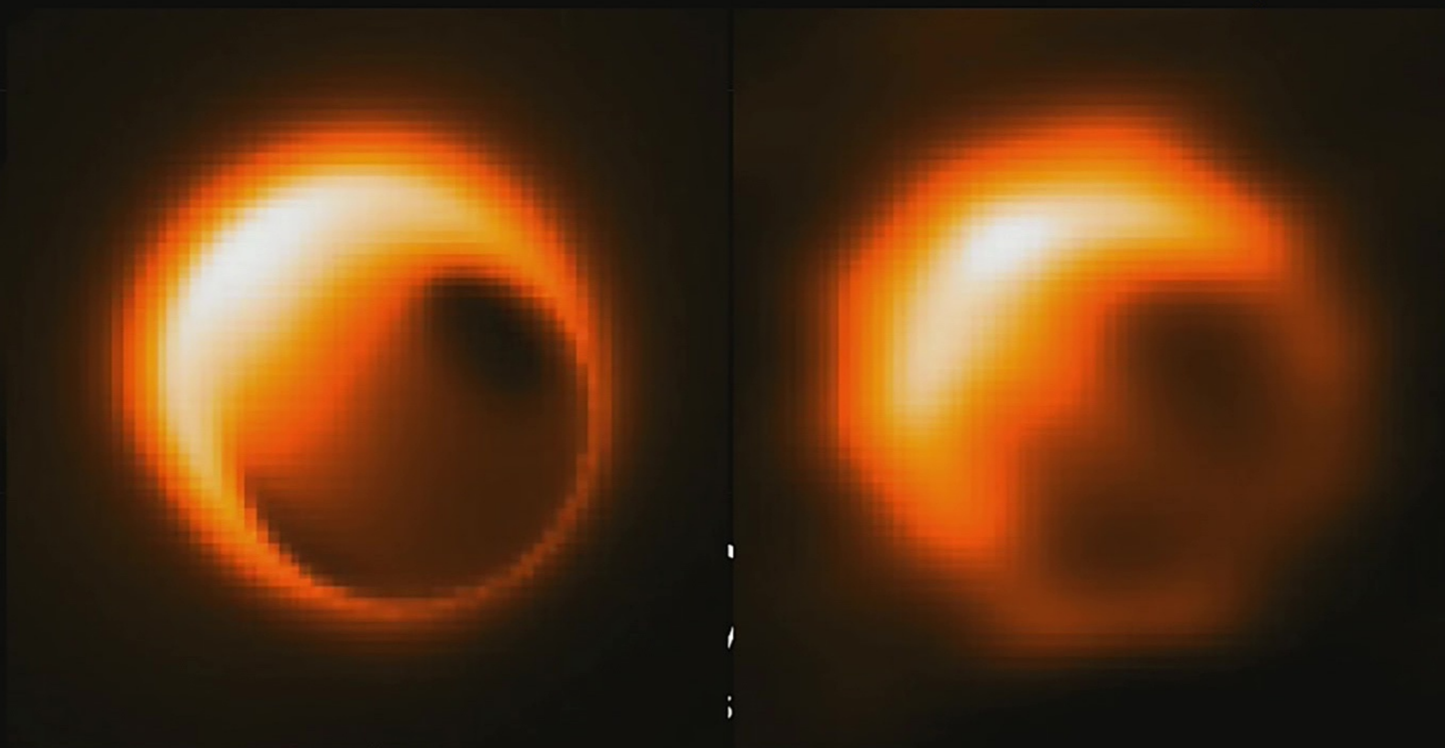

cattering

Fish et al. (2014)

CONVERGENCE

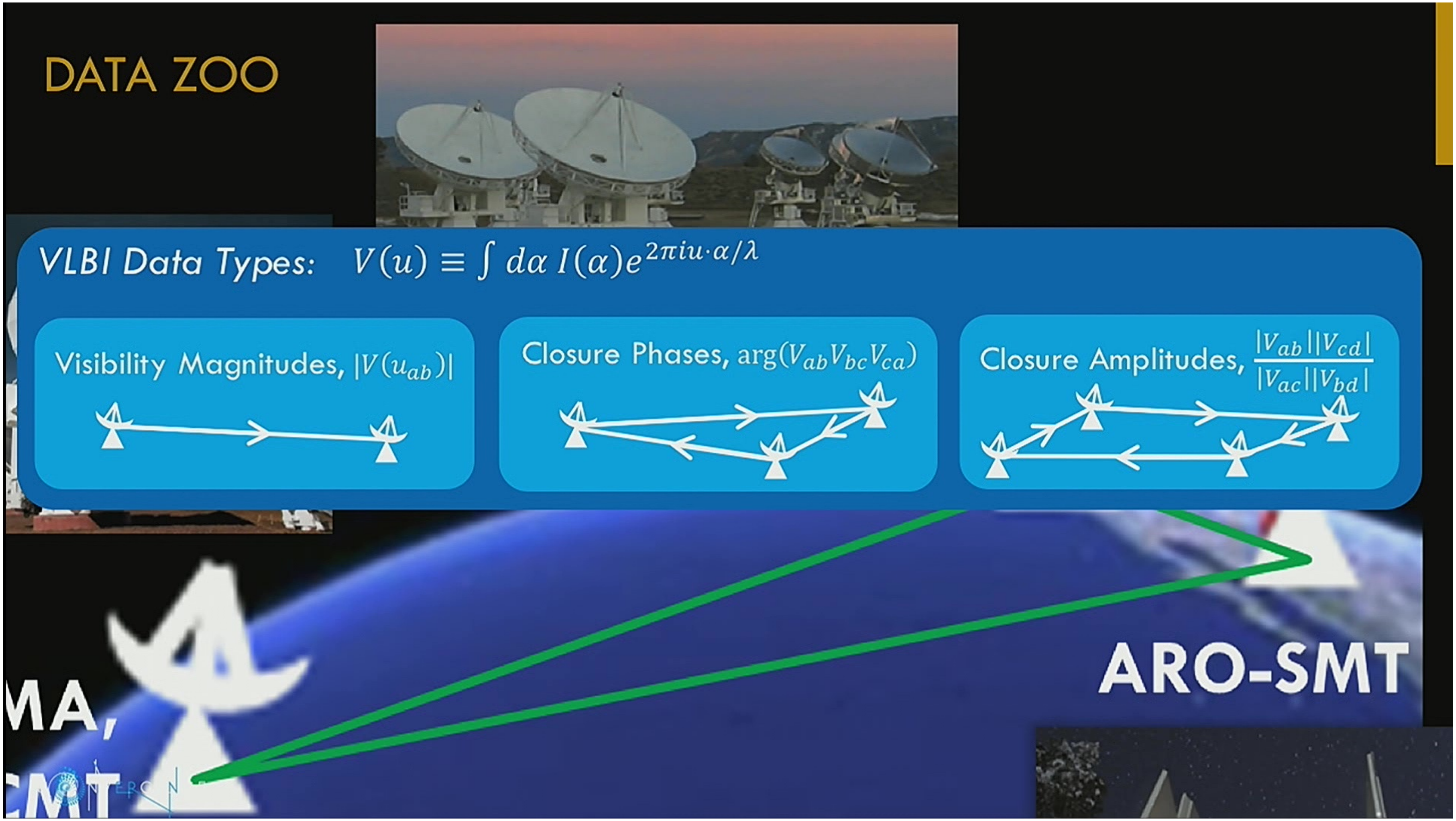
DATA ZOO
VLBI Data Types: $V(u) \equiv \int d\alpha\, I(\alpha) e^{2\pi i u\cdot\alpha/\lambda}$
Visibility Magnitudes, $|V(u_{ab})|$
Closure Phases, $\arg(V_{ab}V_{bc}V_{ca})$
Closure Amplitudes, $\frac{|V_{ab}||V_{cd}|}{|V_{ac}||V_{bd}|}$
ARO-SMT

DATA ZOO

VLBI Data Types: $V(u) \equiv \int d\alpha\, I(\alpha) e^{2\pi i u \cdot \alpha/\lambda}$

- Visibility Magnitudes, $|V(u_{ab})|$
- Closure Phases, $\arg(V_{ab}V_{bc}V_{ca})$
- Closure Amplitudes, $\frac{|V_{ab}||V_{cd}|}{|V_{ac}||V_{bd}|}$

Stokes Parameters:

- I ↕ + ↔
- Q ↕ - ↔
- U ↘ - ↗
- V ↻ - ↺

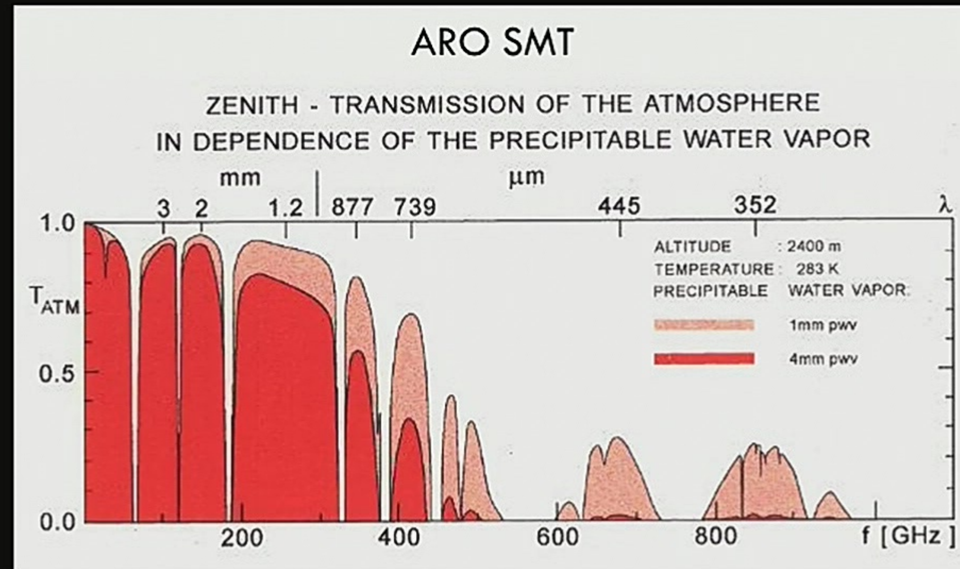

Frequency:

- 230 GHz (1.3 mm)
- 345 GHz (0.87 mm)
- ...

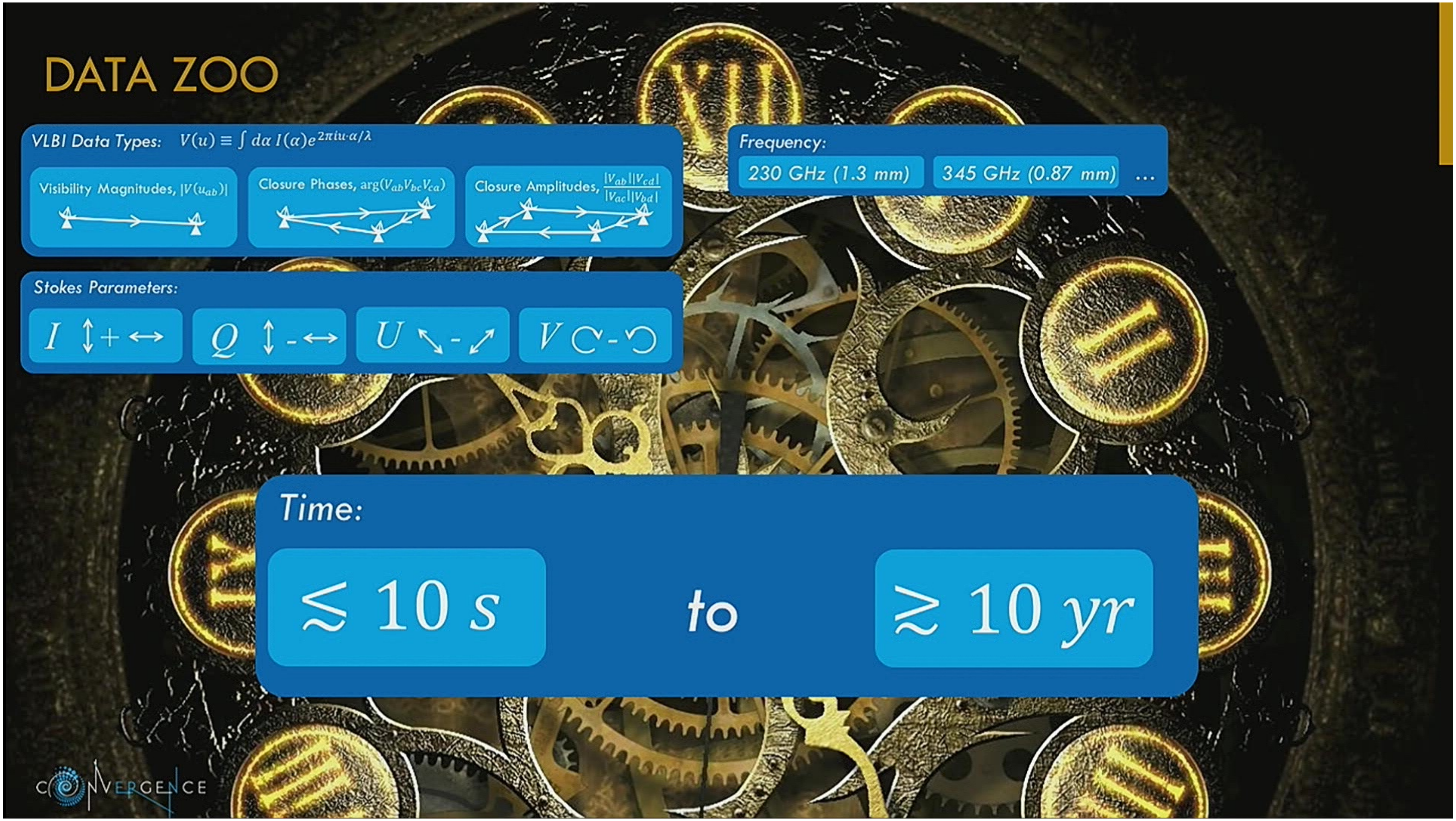
DATA ZOO
VLBI Data Types: $V(u) \equiv \int d\alpha\, I(\alpha) e^{2\pi i u\cdot\alpha/\lambda}$
Visibility Magnitudes, $|V(u_{ab})|$
Closure Phases, $\arg(V_{ab}V_{bc}V_{ca})$
Closure Amplitudes, $\frac{|V_{ab}||V_{cd}|}{|V_{ac}||V_{bd}|}$
Frequency:
230 GHz (1.3 mm)
345 GHz (0.87 mm)
…
Stokes Parameters:
I ↕ + ↔
Q ↕ - ↔
U ↘ - ↗
V ↻ - ↺
Time:
$\lesssim 10\ s$
to
$\gtrsim 10\ yr$
CONVERGENCE

DATA ZOO

VLBI Data Types: $V(u) \equiv \int d\alpha\, I(\alpha) e^{2\pi i u \cdot \alpha / \lambda}$

- Visibility Magnitudes, $|V(u_{ab})|$
- Closure Phases, $\arg(V_{ab}V_{bc}V_{ca})$
- Closure Amplitudes, $\frac{|V_{ab}||V_{cd}|}{|V_{ac}||V_{bd}|}$

Stokes Parameters:

I ↕ + ↔ | Q ↕ - ↔ | U ↘ - ↗ | V ↻ - ↺

Frequency:

230 GHz (1.3 mm) | 345 GHz (0.87 mm) | …

Time:

$\lesssim 10\ s$ to $\gtrsim 10\ yr$

Sources:

- *Sagittarius A* (Galactic Center)*
- *M87 (Center of Virgo Cluster)*
- …

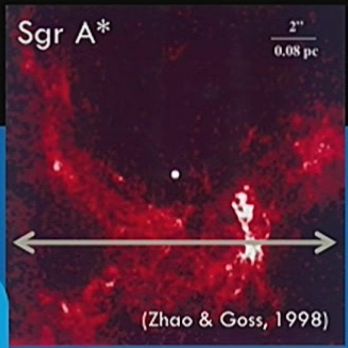

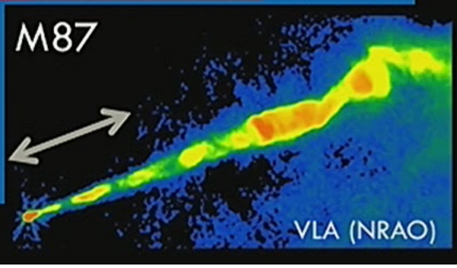

CONVERGENCE

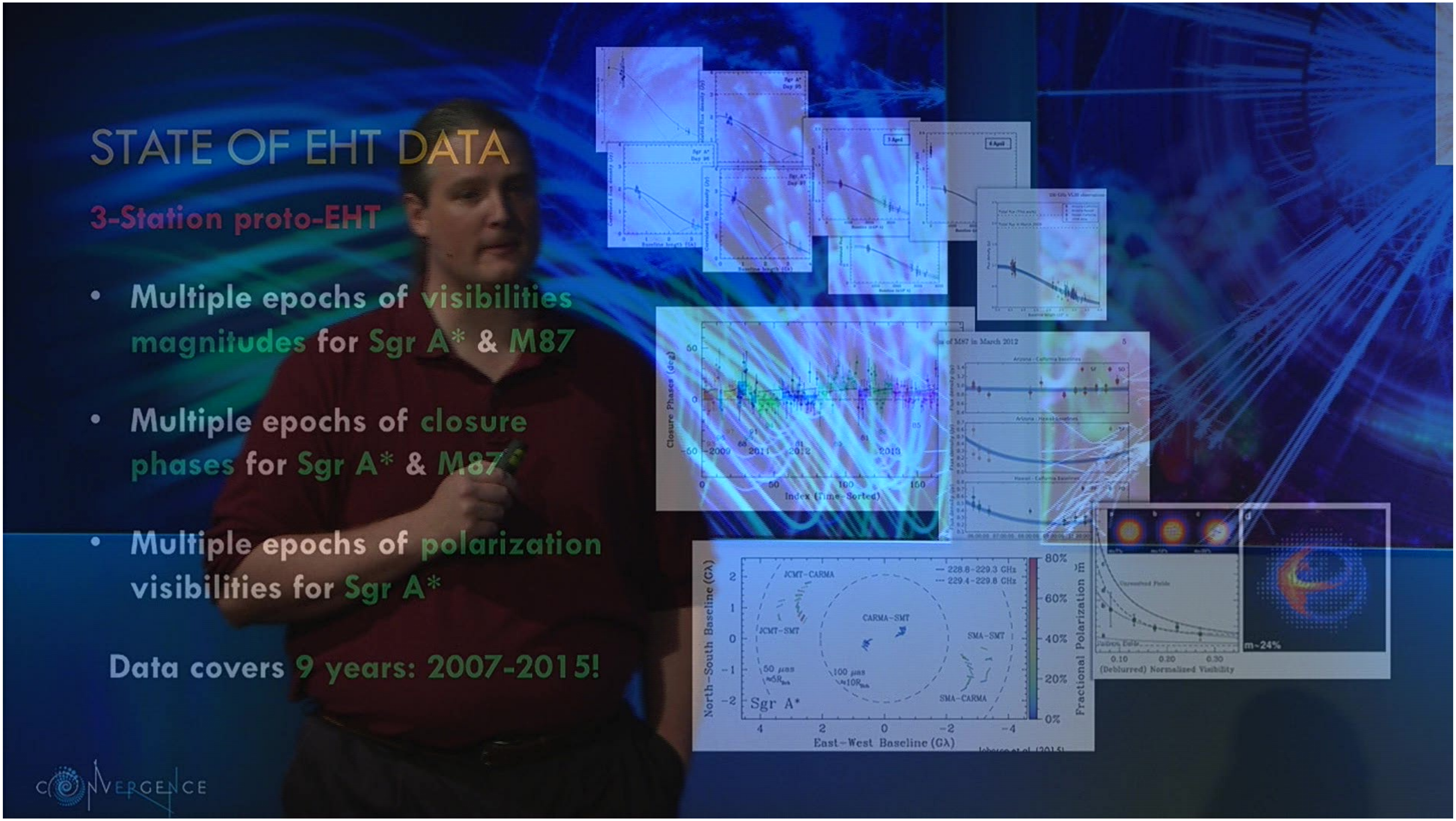
STATE OF EHT DATA
3-Station proto-EHT
• Multiple epochs of visibilities magnitudes for Sgr A* & M87
• Multiple epochs of closure phases for Sgr A* & M87
• Multiple epochs of polarization visibilities for Sgr A*
Data covers 9 years: 2007-2015!
Closure Phases (deg)
Index (Time-Sorted)
North-South Baseline (Gλ)
East-West Baseline (Gλ)
Fractional Polarization
JCMT-CARMA
JCMT-SMT
CARMA-SMT
SMA-SMT
SMA-CARMA
Sgr A*
(Deblurred) Normalized Visibility
CONVERGENCE

STATE OF EHT DATA

3-Station proto-EHT

- **Multiple epochs of visibilities magnitudes for Sgr A* & M87**
- **Multiple epochs of closure phases for Sgr A* & M87**
- **Multiple epochs of polarization visibilities for Sgr A***

Data covers 9 years: 2007-2015!

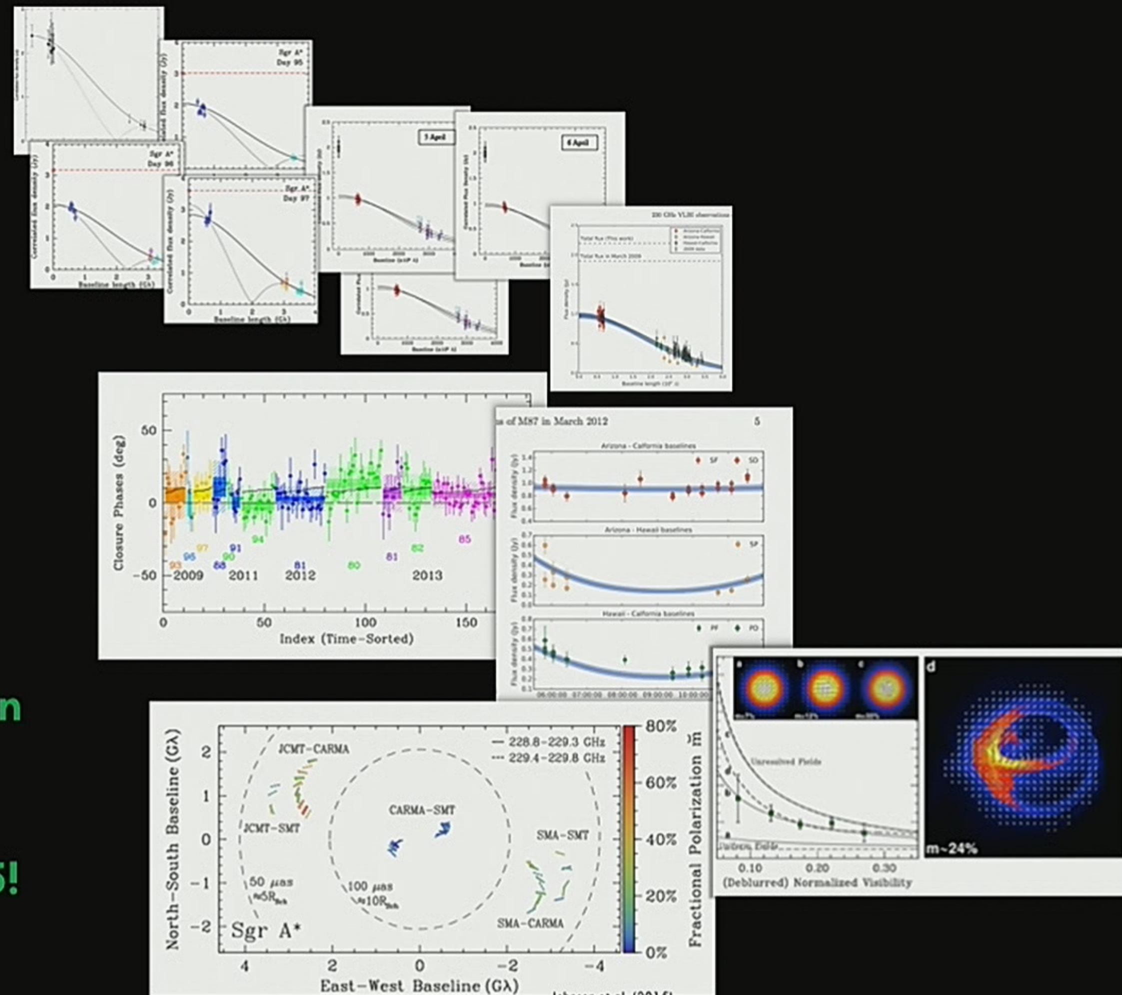

CONVERGENCE

INCOMPLETENESS

Observational:

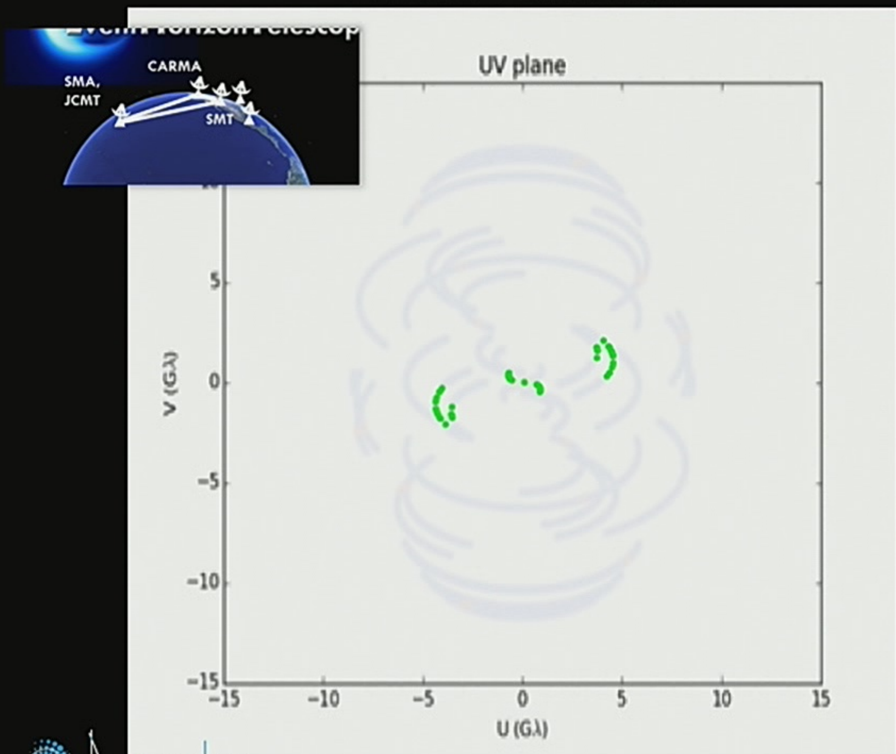

Theoretical:

Key known unknowns:

- **Geometry & Dynamics of emission region**

LESSONS FROM PRECISION COSMOLOGY

Table 9. Parameter 68 % confidence levels for the base ΛCDM cosmology computed from the *Planck* CMB power spectra, in combination with the CMB lensing likelihood ("lensing").

Parameter	*Planck* TT+lowP+lensing
$\Omega_b h^2$	0.02226 ± 0.00023
$\Omega_c h^2$	0.1186 ± 0.0020
$100\theta_{MC}$	1.04103 ± 0.00046
τ	0.066 ± 0.016
$\ln(10^{10} A_s)$	3.062 ± 0.029
n_s	0.9677 ± 0.0060

LESSONS FROM PRECISION COSMOLOGY

Planck Collaboration: Diffuse component separation: Foreground maps

Table 4. Summary of main parametric signal models for the temperature analysis. For polarization, the same parametric functions are employed, but only CMB, synchrotron, and thermal dust emission are included in the model, with spectral parameters fixed to the result of the temperature analysis. The symbol "~" implies that the respective parameter has a prior as given by the right-hand side distribution; Uni denotes a uniform distribution within the indicated limits, and N denotes a (normal) Gaussian distribution with the indicated mean and standard devation.

Component	Free parameters and priors	Brightness temperature, s_ν [μK_{RJ}]	Additional information
CMB[a]	$A_{cmb} \sim \mathrm{Uni}(-\infty,\infty)$	$x = \frac{h\nu}{k_B T_{CMB}}$ $g(\nu) = (\exp(x)-1)^2/(x^2\exp(x))$ $s_{CMB} = A_{CMB}/g(\nu)$	$T_{CMB} = 2.7255\,\mathrm{K}$
Synchrotron[a]	$A_s > 0$ $\alpha > 0$, spatially constant	$s_s = A_s\left(\frac{\nu_0}{\nu}\right)^2 \frac{f_s(\frac{\nu}{\alpha})}{f_s(\frac{\nu_0}{\alpha})}$	$\nu_0 = 408\,\mathrm{MHz}$ $f_s(\nu)$ = Ext template
Free-free	$\log \mathrm{EM} \sim \mathrm{Uni}(-\infty,\infty)$ $T_e \sim N(7000 \pm 500\,\mathrm{K})$	$g_{ff} = \log\left\{\exp\left[5.960 - \sqrt{3}/\pi \log(\nu_9\, T_4^{-3/2})\right] + e\right\}$ $\tau = 0.05468\, T_e^{-3/2}\, \nu_9^{-2}\, \mathrm{EM}\, g_{ff}$ $s_{ff} = 10^6\, T_e (1 - e^{-\tau})$	$T_4 = T_e/10^4$ $\nu_9 = \nu/(10^9\,\mathrm{Hz})$
Spinning dust........	$A^1_{sd}, A^2_{sd} > 0$ $\nu^2_p \sim N(19 \pm 3\,\mathrm{GHz})$ $\nu^1_p > 0$, spatially constant	$s_{sd} = A_{sd}\cdot\left(\frac{\nu_0}{\nu}\right)^2 \frac{f_{sd}(\nu\cdot\nu_{p0}/\nu_p)}{f_{sd}(\nu_0\cdot\nu_{p0}/\nu_p)}$	$\nu^1_0 = 22.8\,\mathrm{GHz}$ $\nu^2_0 = 41.0\,\mathrm{GHz}$ $\nu_{p0} = 30.0\,\mathrm{GHz}$ $f_{sd}(\nu)$ = Ext template
Thermal dust[a]	$A_d > 0$ $\beta_d \sim N(1.55 \pm 0.1)$ $T_d \sim N(23 \pm 3\,\mathrm{K})$	$\gamma = \frac{h}{k_B T_d}$ $s_d = A_d\cdot\left(\frac{\nu}{\nu_0}\right)^{\beta_d+1} \frac{\exp(\gamma\nu_0)-1}{\exp(\gamma\nu)-1}$	$\nu_0 = 545\,\mathrm{GHz}$
SZ	$y_{sz} > 0$	$s_{sz} = 10^6\, y_{sz}/g(\nu)\, T_{CMB}\left(\frac{x(\exp(x)+1)}{\exp(x)-1} - 4\right)$	
Line emission	$A_i > 0$ $h_{ij} > 0$, spatially constant	$s_i = A_i h_{ij} \frac{F_i(\nu_j)}{F_i(\nu_0)} \frac{g(\nu_0)}{g(\nu_j)}$	$i \in$ {CO $J=1\to0$, CO $J=2\to1$, CO $J=3\to2$, 94/100} j = detector index F = unit conversion

[a] Polarized component.

Planck Collaboration: Diffuse component separation: Foreground maps

Table 5. Summary of full-sky foreground products available from the PLA. Each entry in the first column corresponds to one multi-column and (optionally) multi-extension FITS file, named `COM_CompMap_{label}-commander_{nside}_R2.00.fits`. The various columns in each extension list the posterior maximum, mean, and rms maps, in that order, when available. The values reported in columns 5 to 7 in this table are the mean and standard deviations of these posterior statistic maps.

File	FITS extension	Parameter	ν_{ref} [GHz/band]	Posterior outside LM93: P_{max}	Posterior outside LM93: Mean	Posterior outside LM93: RMS	Unit
TEMPERATURE AT 1° FWHM, N_{side} = 256							
AME	0	A_{sd1}	22.8	93 ± 118	92 ± 118	11 ± 3	μK_{RJ}
		ν_{sd1}	...	19 ± 1	19 ± 1	2.0 ± 0.8	GHz
	1	A_{sd2}	41	14 ± 21	18 ± 22	4.1 ± 2.8	μK_{RJ}
CMB	0	A_{cmb}	...	3 ± 67	3 ± 67	1.5 ± 0.8	μK_{cmb}
CO	0	A_{CO10}	100-ds1	0.3 ± 1.3	0.4 ± 1.3	0.06 ± 0.05	$K_{RJ}\,\mathrm{km\,s^{-1}}$
	1	A_{CO21}	217-1	0.22 ± 0.57	0.29 ± 0.57	0.04 ± 0.01	$K_{RJ}\,\mathrm{km\,s^{-1}}$
	2	A_{CO32}	353-ds2	0.16 ± 0.21	0.26 ± 0.26	0.05 ± 0.01	$K_{RJ}\,\mathrm{km\,s^{-1}}$
dust	0	A_d	545	163 ± 228	163 ± 228	0.66 ± 0.11	μK_{RJ}
		T_d	...	21 ± 2	21 ± 2	1.1 ± 0.7	K
		β_d	...	1.53 ± 0.05	1.51 ± 0.06	0.05 ± 0.03	...
freefree	0	EM	...	15 ± 35	13 ± 35	2.3 ± 2.4	$\mathrm{cm^{-6}\,pc}$
		T_e	...	7000 ± 11	7000 ± 11	...	K
Synchrotron	0	A_s	0.408	20 ± 15	20 ± 15	1.1 ± 0.2	K^a_{RJ}
SZ	0	A_{sz}	...	1.4 ± 1.4[b]	2.0 ± 1.3[b]	0.8 ± 0.2[b]	$10^{-6}\,y_{sz}$
xline[c]	0	$A_{94/100}$	100-ds1	0.09 ± 0.06	0.9 ± 0.8	0.7 ± 0.6	μK_{cmb}
TEMPERATURE AT 7.5 FWHM, N_{side} = 2048							
CO21[d]	0	A_{CO21}	217-1	0.2 ± 0.8	...	...	$K_{RJ}\,\mathrm{km\,s^{-1}}$
ThermalDust[d]	0	A_d	545	0.2 ± 0.8	...	...	μK_{RJ}
		β_d	...	1.54 ± 0.07	...	...	...
POLARIZATION AT 40′ FWHM, N_{side} = 256							
SynchrotronPol[d]	0	P^e_s	30	12 ± 9	...	...	μK_{RJ}
POLARIZATION AT 10′ FWHM, N_{side} = 1024							
DustPol[d]	0	P^e_d	353	8 ± 10	...	...	μK_{RJ}

[a] The data file unit is μK_{RJ} but for convenience we list numbers in K_{RJ} in this table.
[b] Evaluated only over the Coma and Virgo regions.
[c] This is the 94/100 GHz line emission component.
[d] Only the full-mission maps are summarized in this table, but the data files also include corresponding maps for half-mission, half-year, and half-ring data splits.
[e] Data files contains Stokes Q and U parameters, not the polarization amplitude, $P = \sqrt{Q^2 + U^2}$, listed here.

CONVERGENCE

DO EVENT HORIZONS EXIST?

- **Testing robust prediction of GR *and* others!**

- **Constrains alternatives to surface of "no" return**

DO EVENT HORIZONS EXIST?

- **Testing robust prediction of GR *and* others!**
- **Constrains alternatives to surface of "no" return**

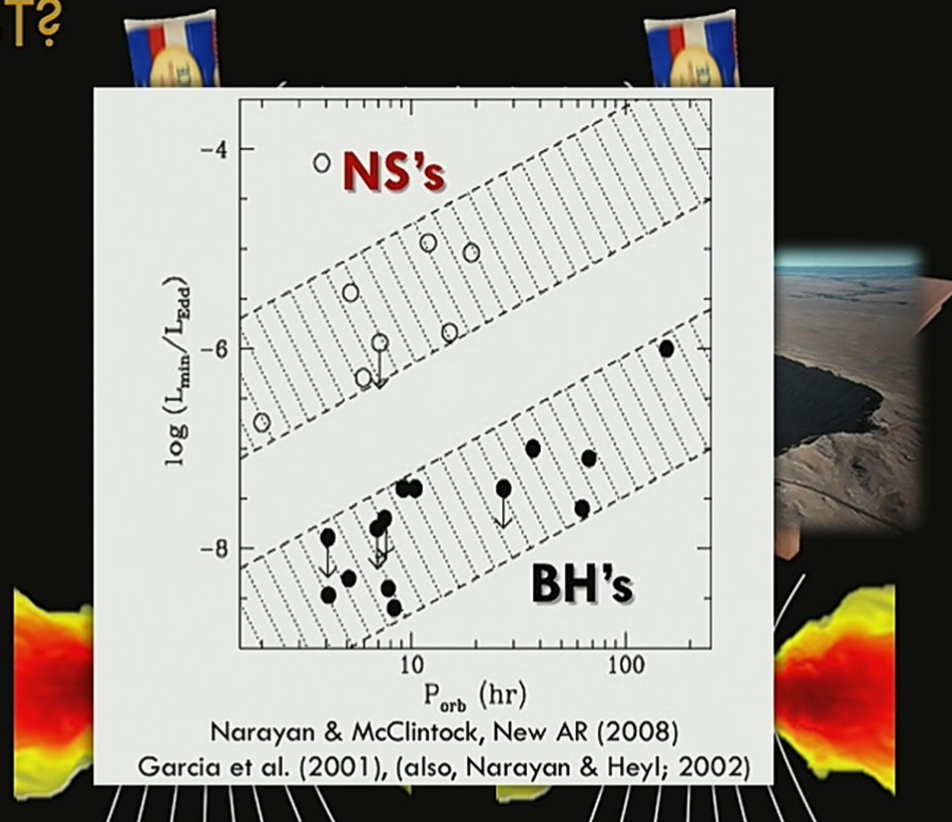

Narayan & McClintock, New AR (2008)
Garcia et al. (2001), (also, Narayan & Heyl; 2002)

$L_{jet} \approx \epsilon_{jet} \dot{M} c^2$
$\epsilon_{jet} \approx 2$

$L_{surf} \approx \dot{M} c^2$
$\approx L_{jet}/\epsilon_{jet}$

THE SIZES OF ASTROPHYSICAL BLACK HOLES

Sgr A*

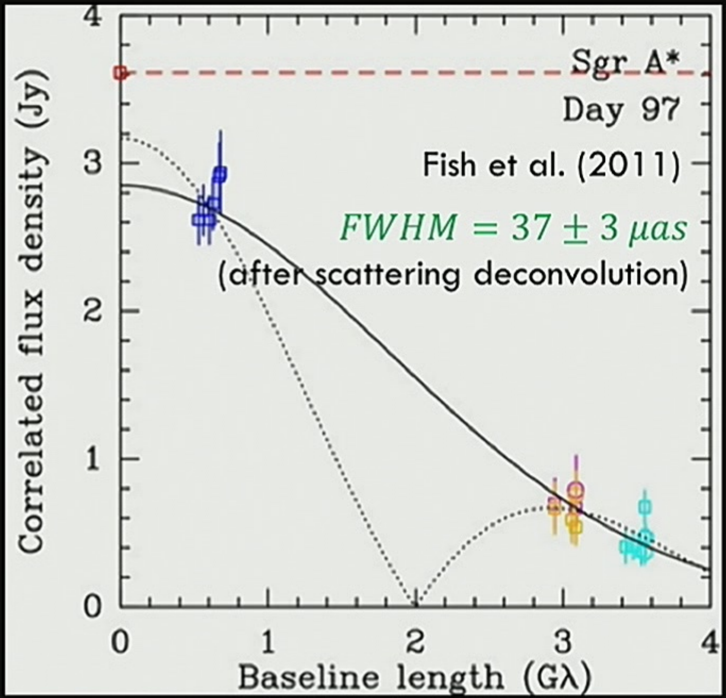

M87

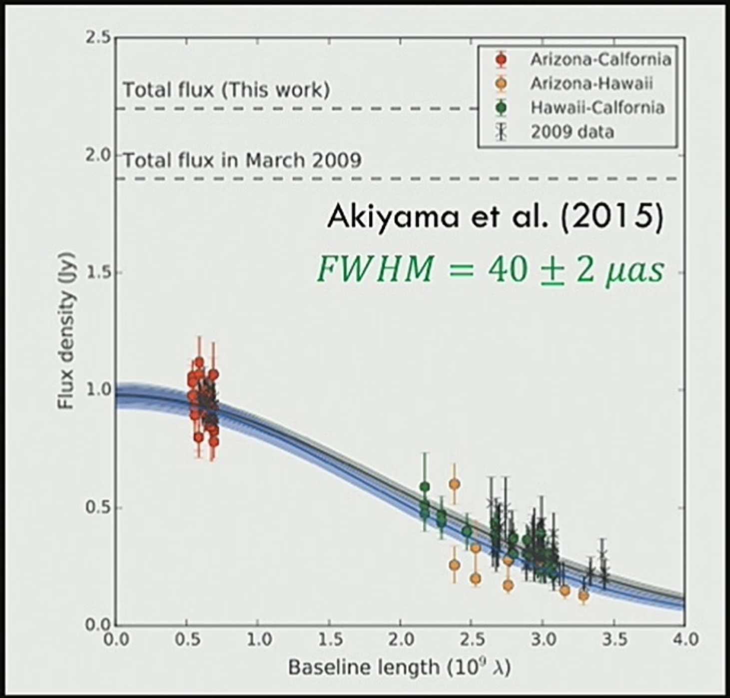

CONVERGENCE

EHT + INFRARED ASTRONOMY:
AT LEAST TWO HORIZONS DO EXIST! (SEE FINE PRINT)

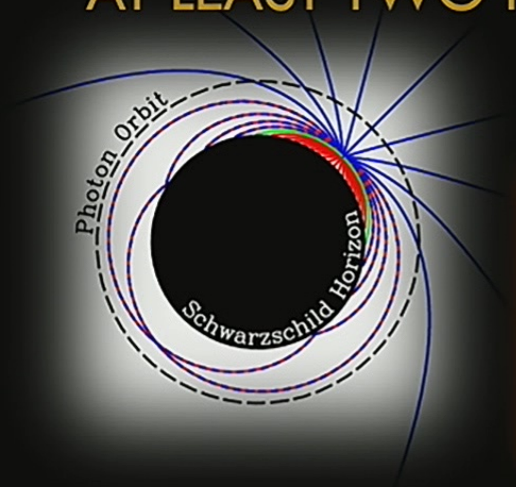

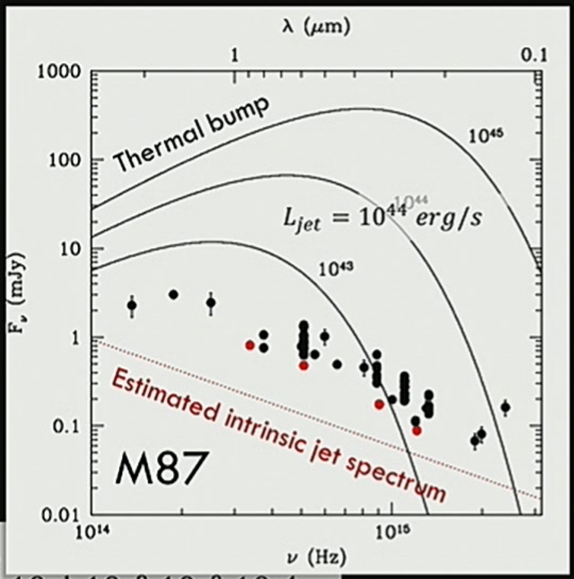

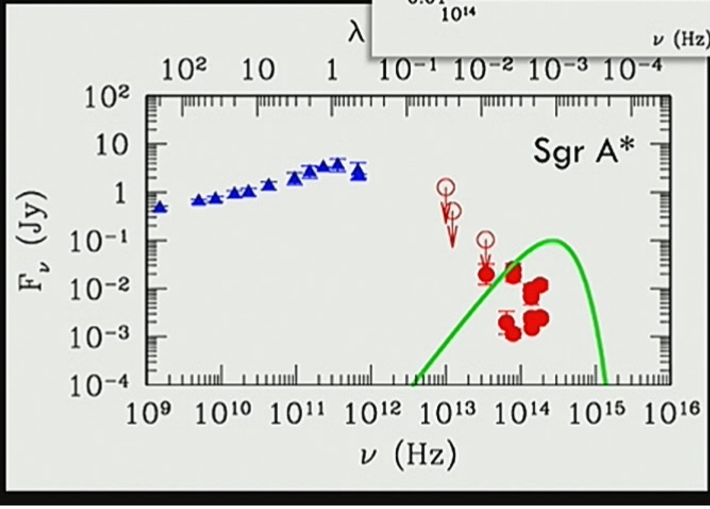

EHT + INFRARED ASTRONOMY:
AT LEAST TWO HORIZONS DO EXIST! (SEE FINE PRINT)

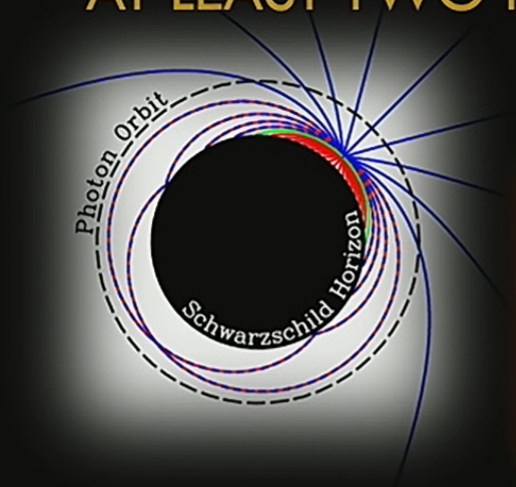

Blackbody Cavity

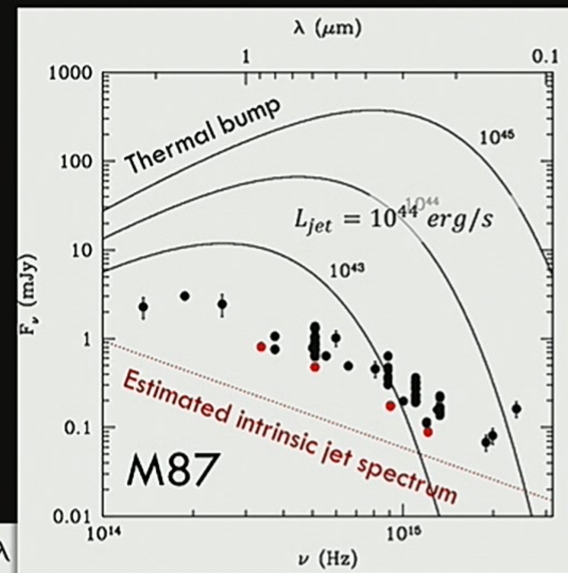

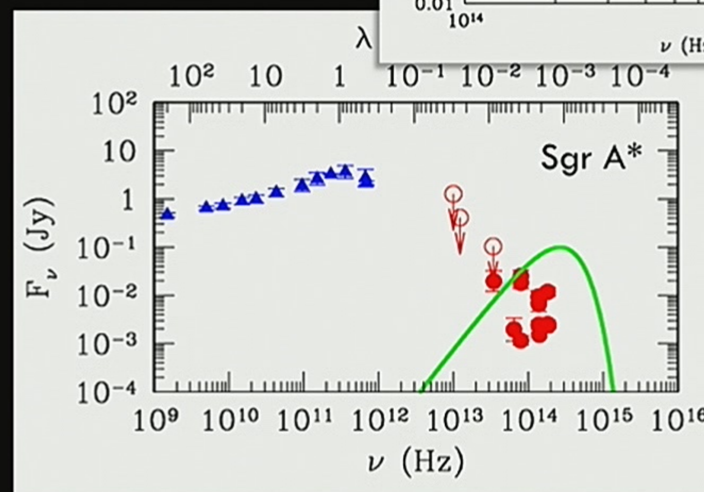

CONVERGENCE

MODELING SGR A*: ACCRETION DISKS

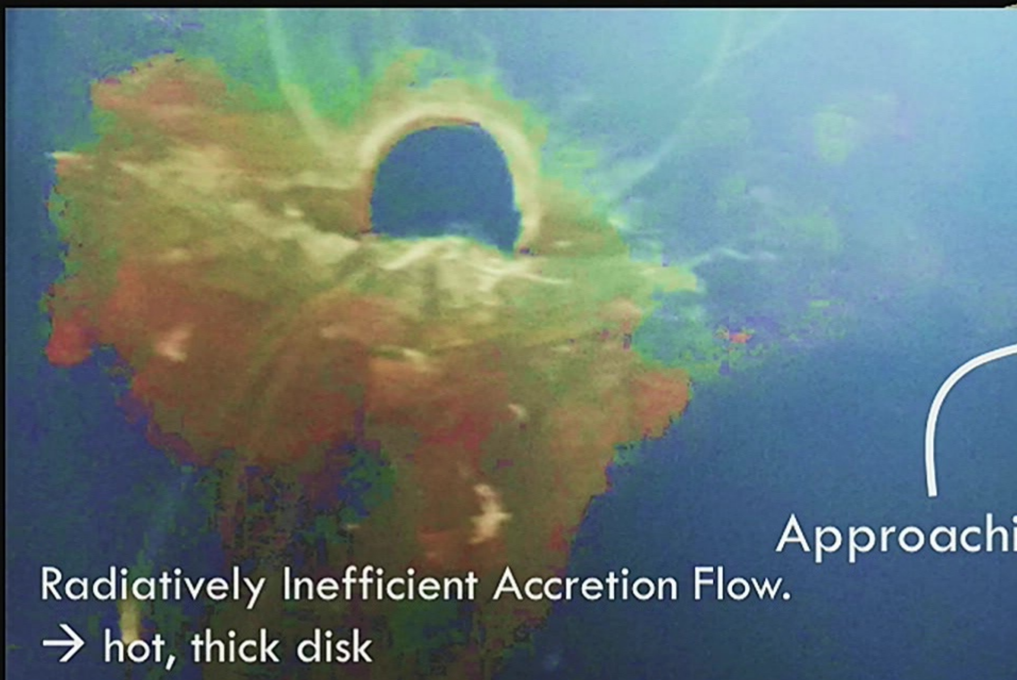

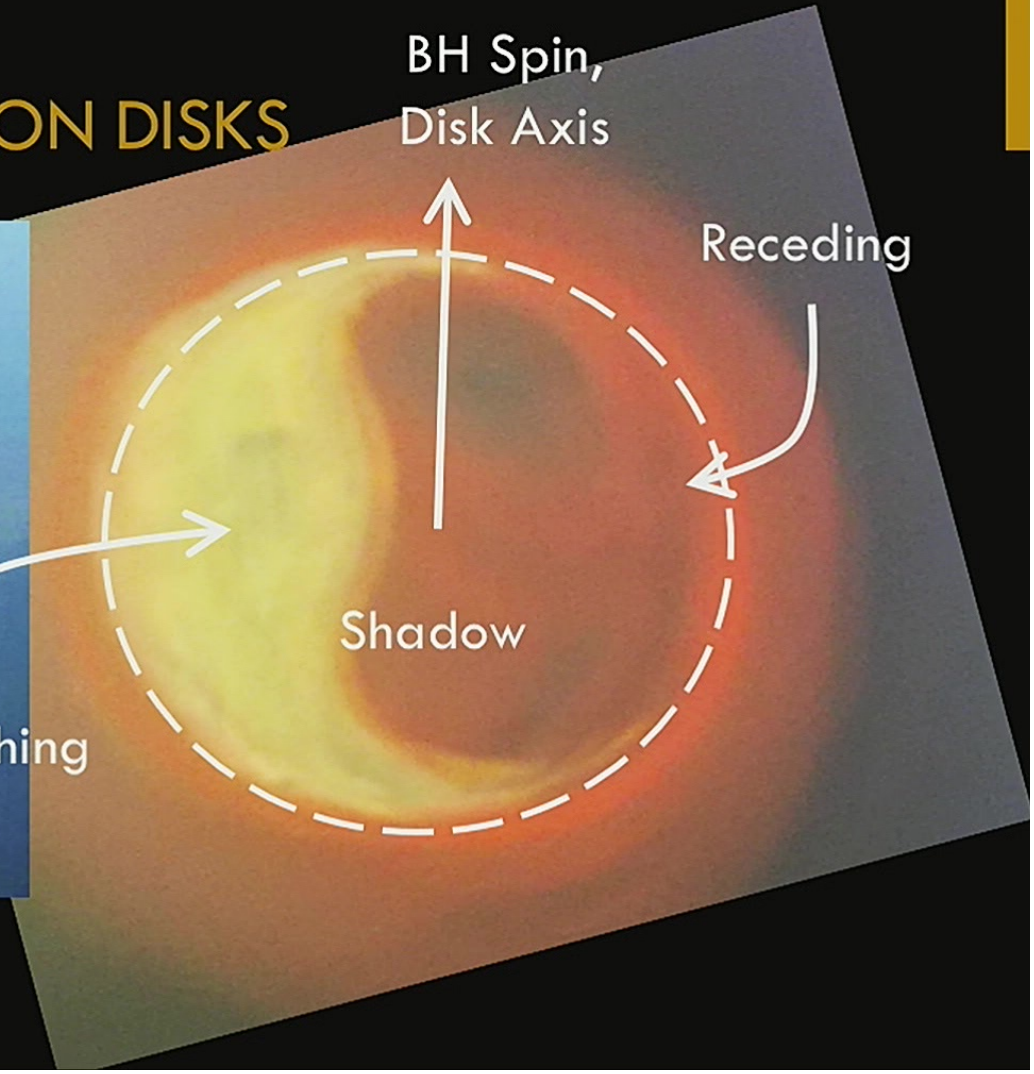

CONVERGENCE

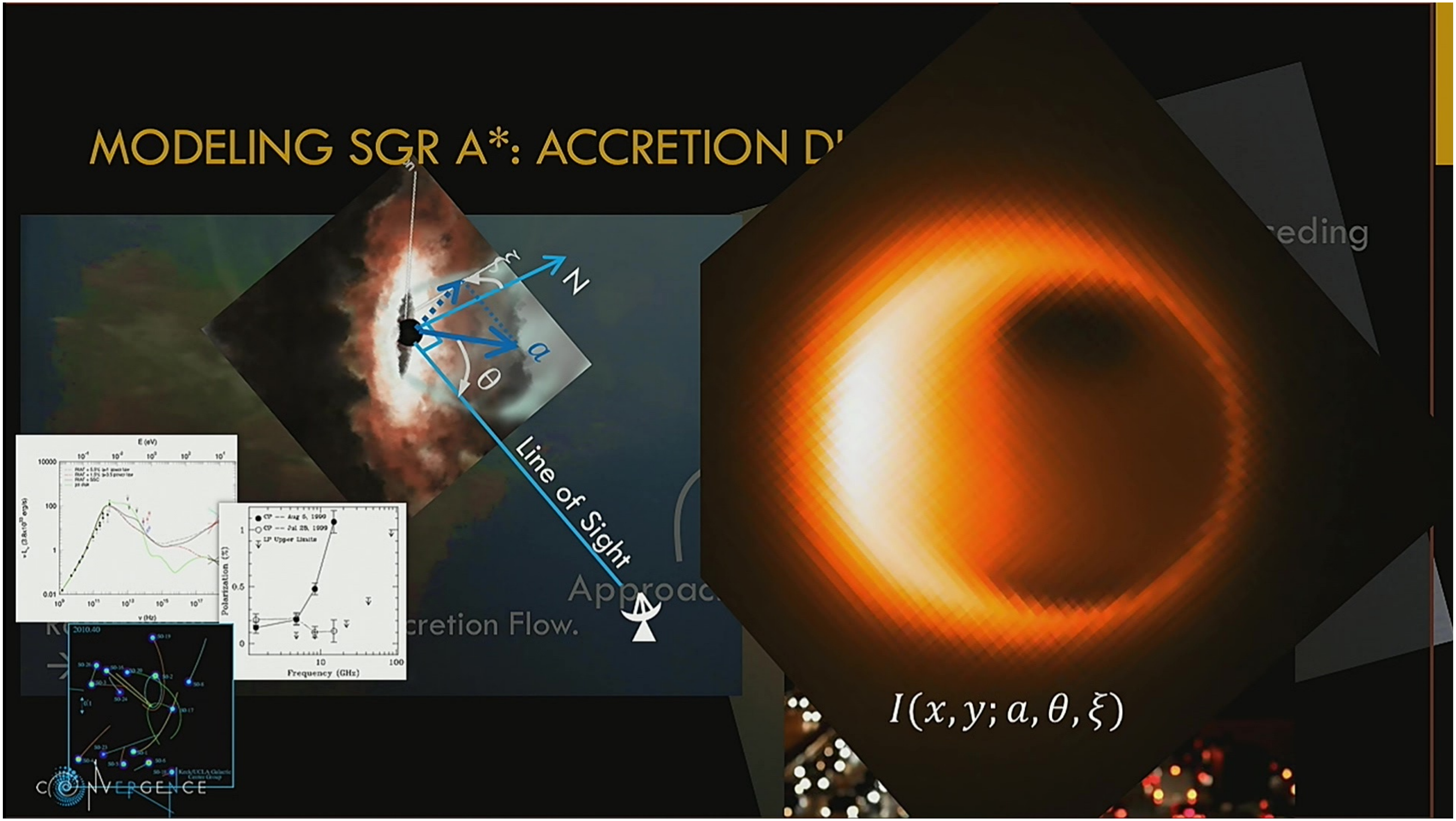
MODELING SGR A*: ACCRETION D
N
a
θ
Line of Sight
Approac
cretion Flow.
eding
I(x,y;a,θ,ξ)
E (eV)
ν (Hz)
Polarization (%)
Frequency (GHz)
CP — Aug 5, 1999
CP — Jul 28, 1999
LP Upper Limits
2010.40
CONVERGENCE

ORIENTATION AND THE GALACTIC CENTER STORY

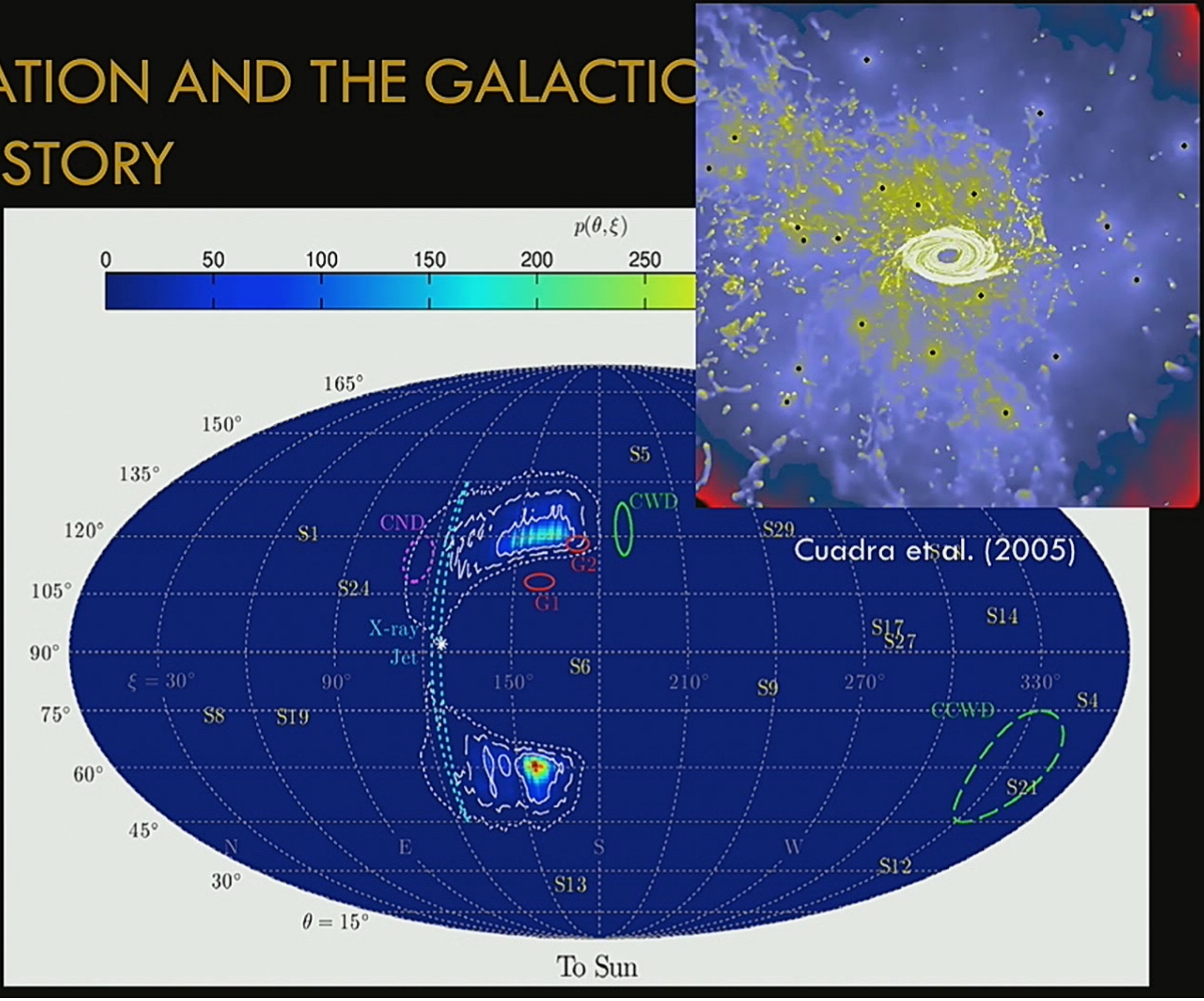

Cuadra et al. (2005)

PROBING ACCRETION WITH 7 YEARS OF EHT DATA

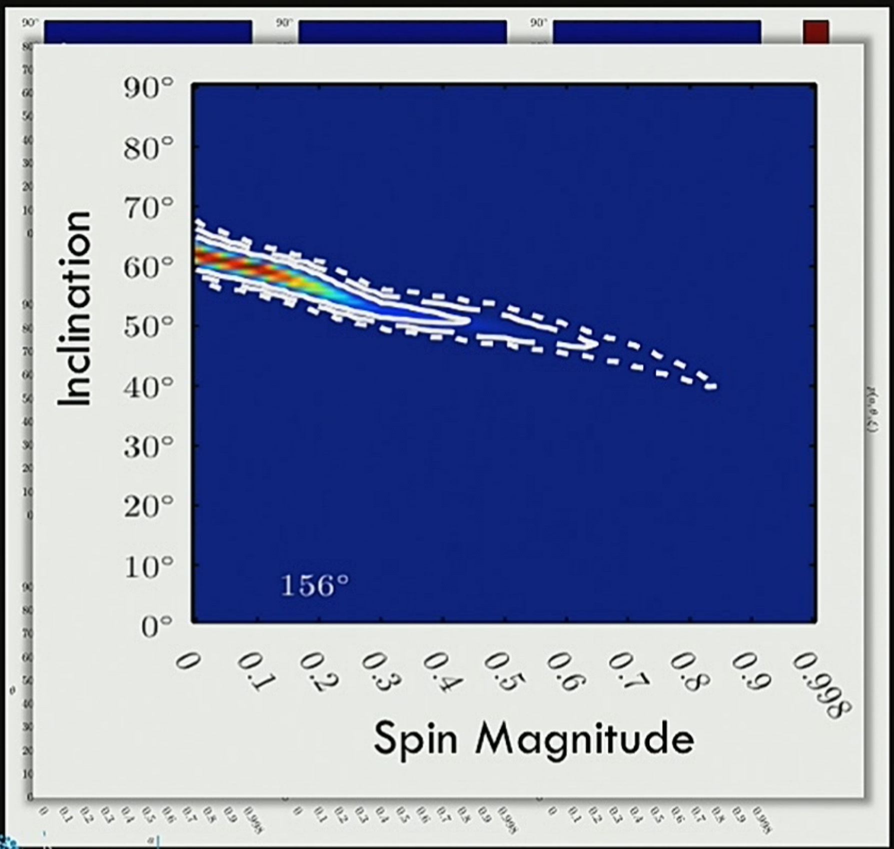

CONVERGENCE

PROBING ACCRETION WITH 7 YEARS OF EHT DATA

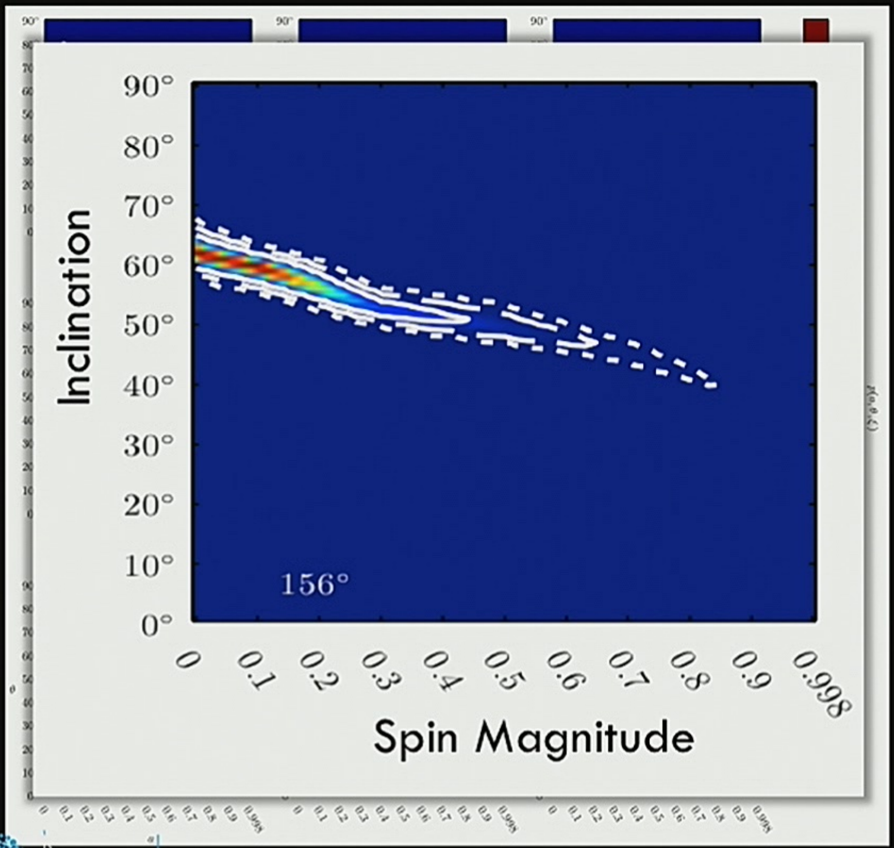

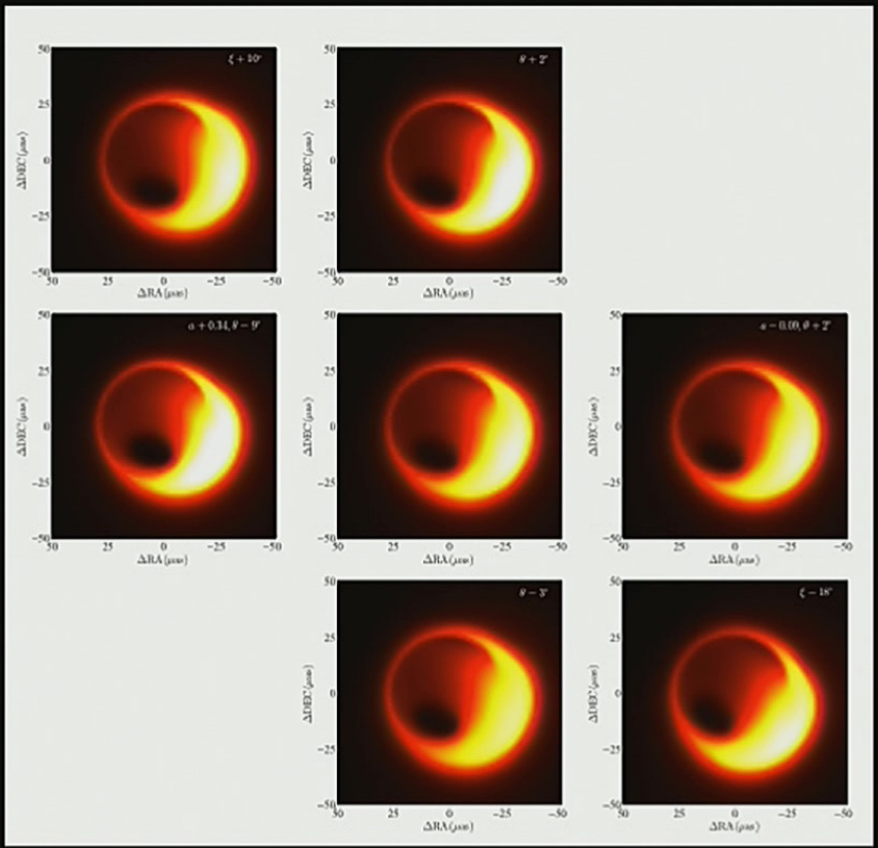

PROBING ACCRETION WITH 7 YEARS OF EHT DATA

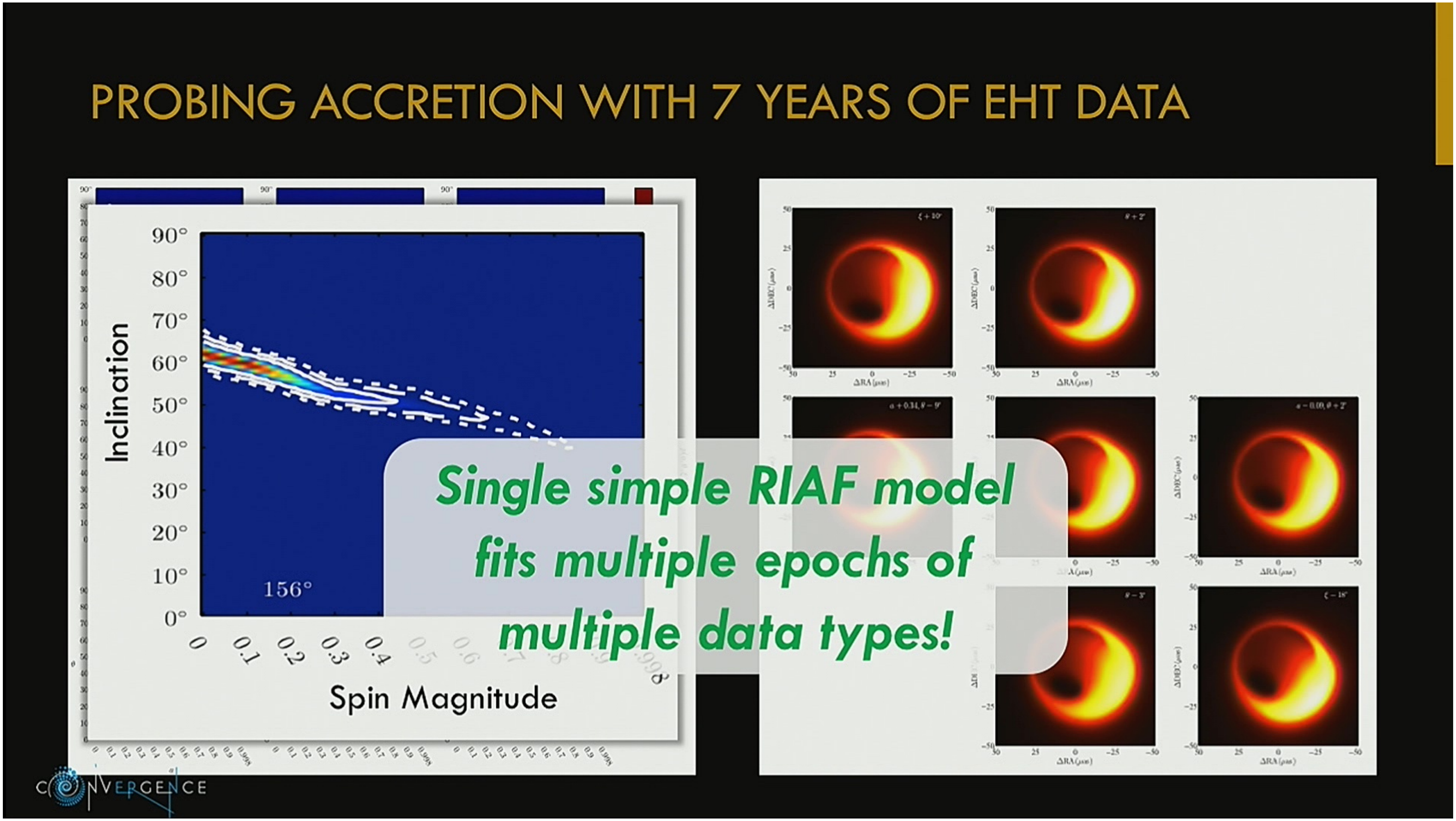

SMALL-SCALE STRUCTURE BUDGET

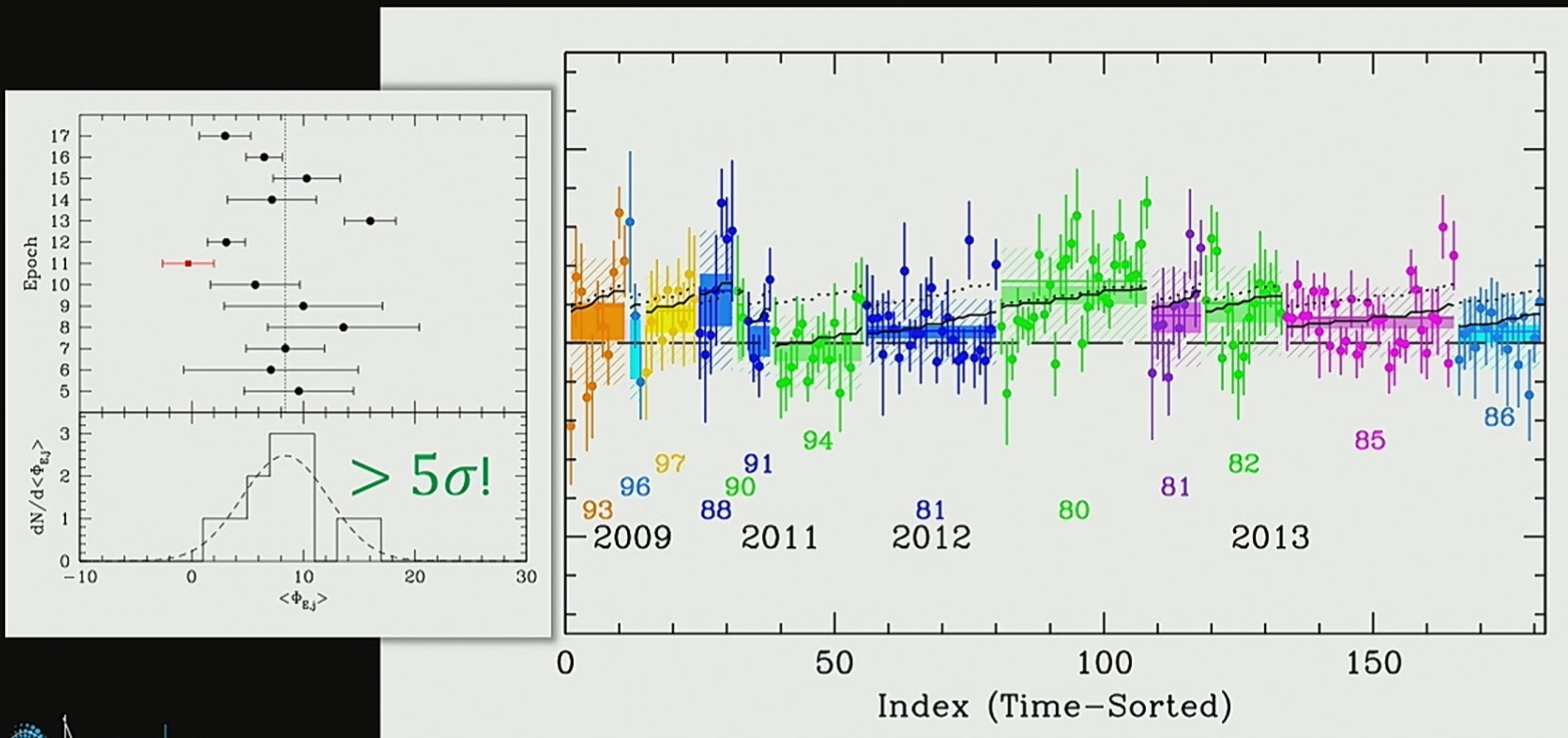

SMALL-SCALE STRUCTURE BUDGET

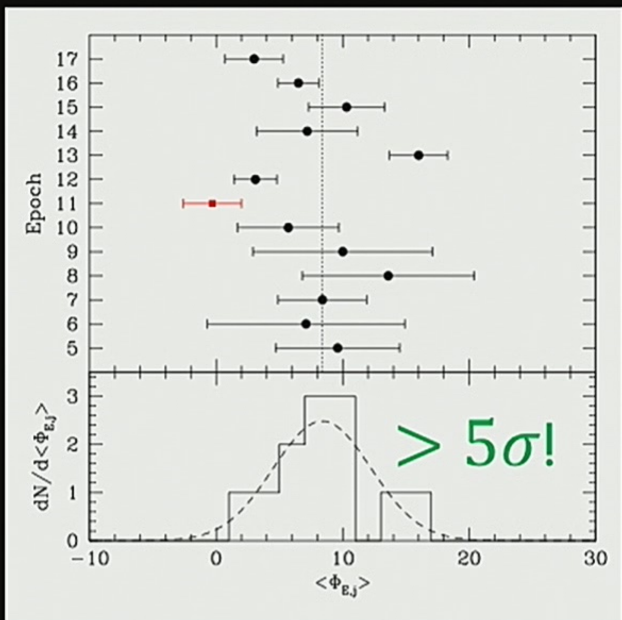

Refractive Scintillation

Galactic "Seeing"

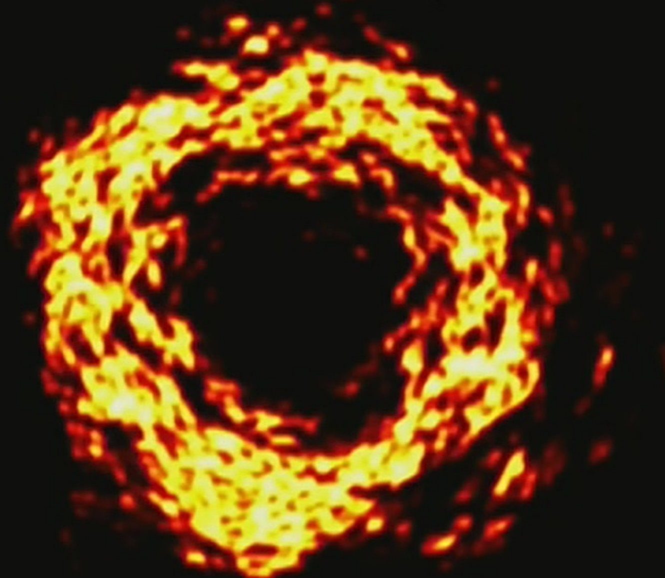

Courtesy of Michael D Johnson

EXPLOITING A DECADE OF EHT OBSERVATION: HUNTING LENSE-THIRRING

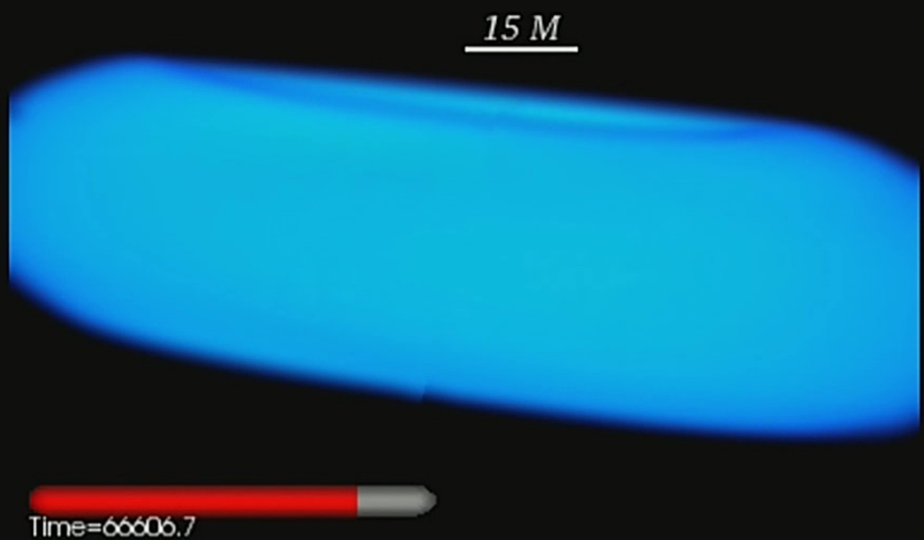

Courtesy of Chris Fragile

EXPLOITING A DECADE OF EHT OBSERVATION: HUNTING LENSE-THIRRING

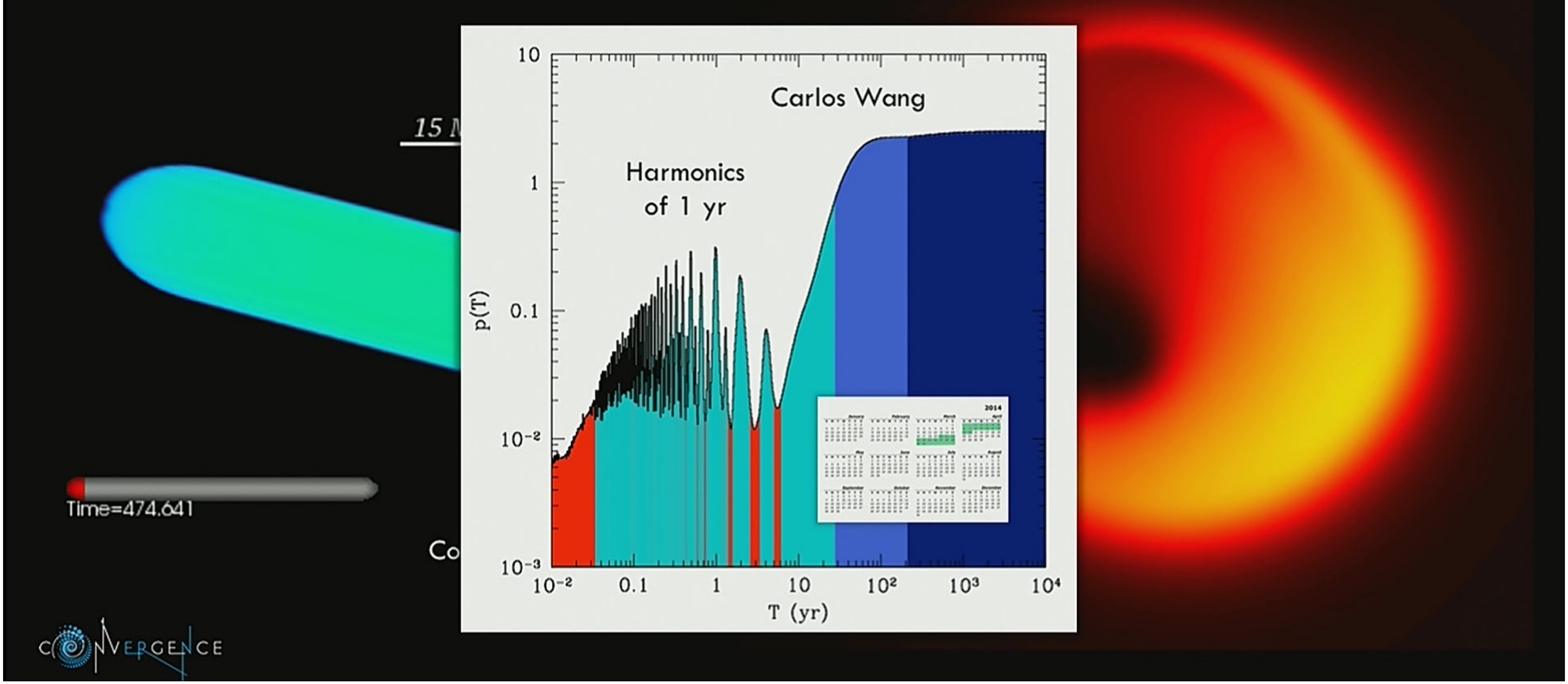

A MATTER OF MASS & DISTANCE: CRITICAL TESTS OF STRONG FIELD GRAVITY

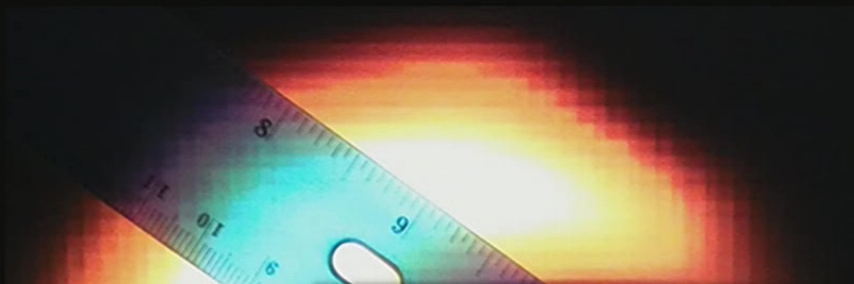

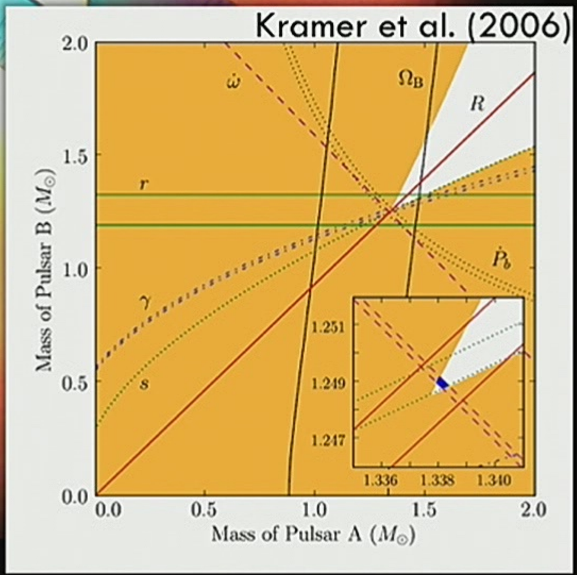

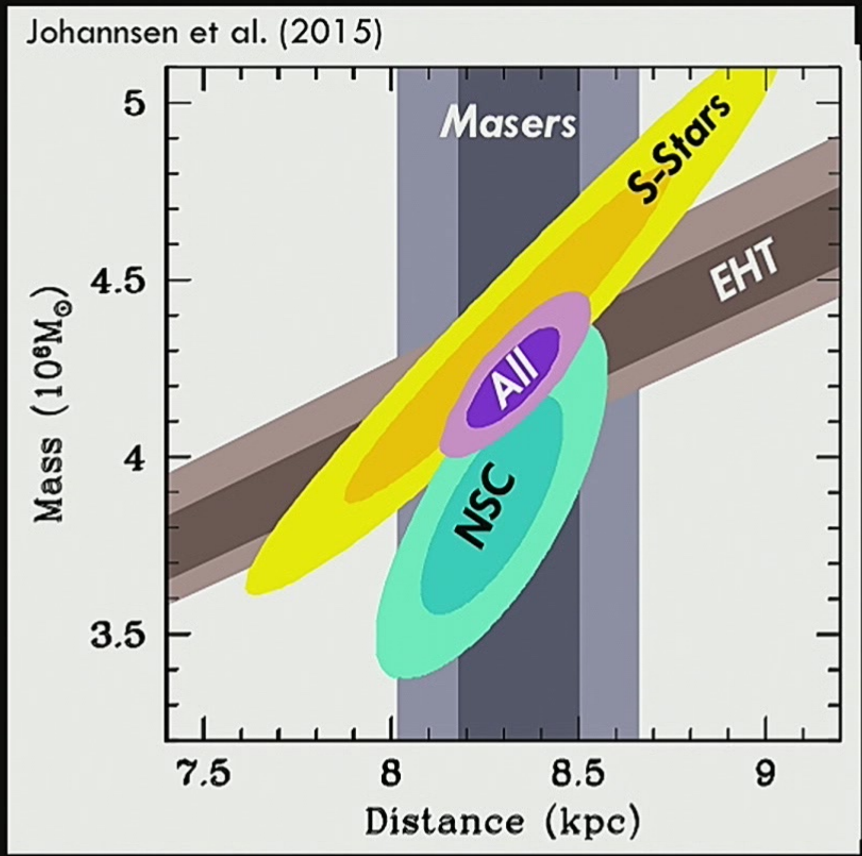

THE SHAPE OF SPACETIME I: HAIRY MULTIPOLES

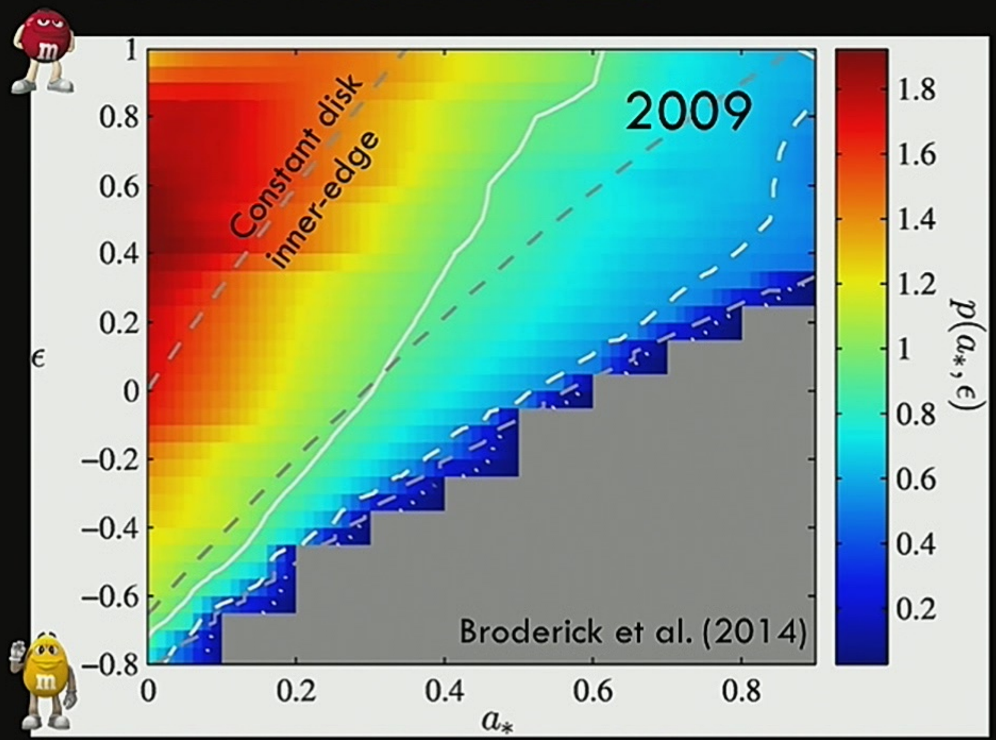

THE SHAPE OF SPACETIME I: HAIRY MULTIPOLES

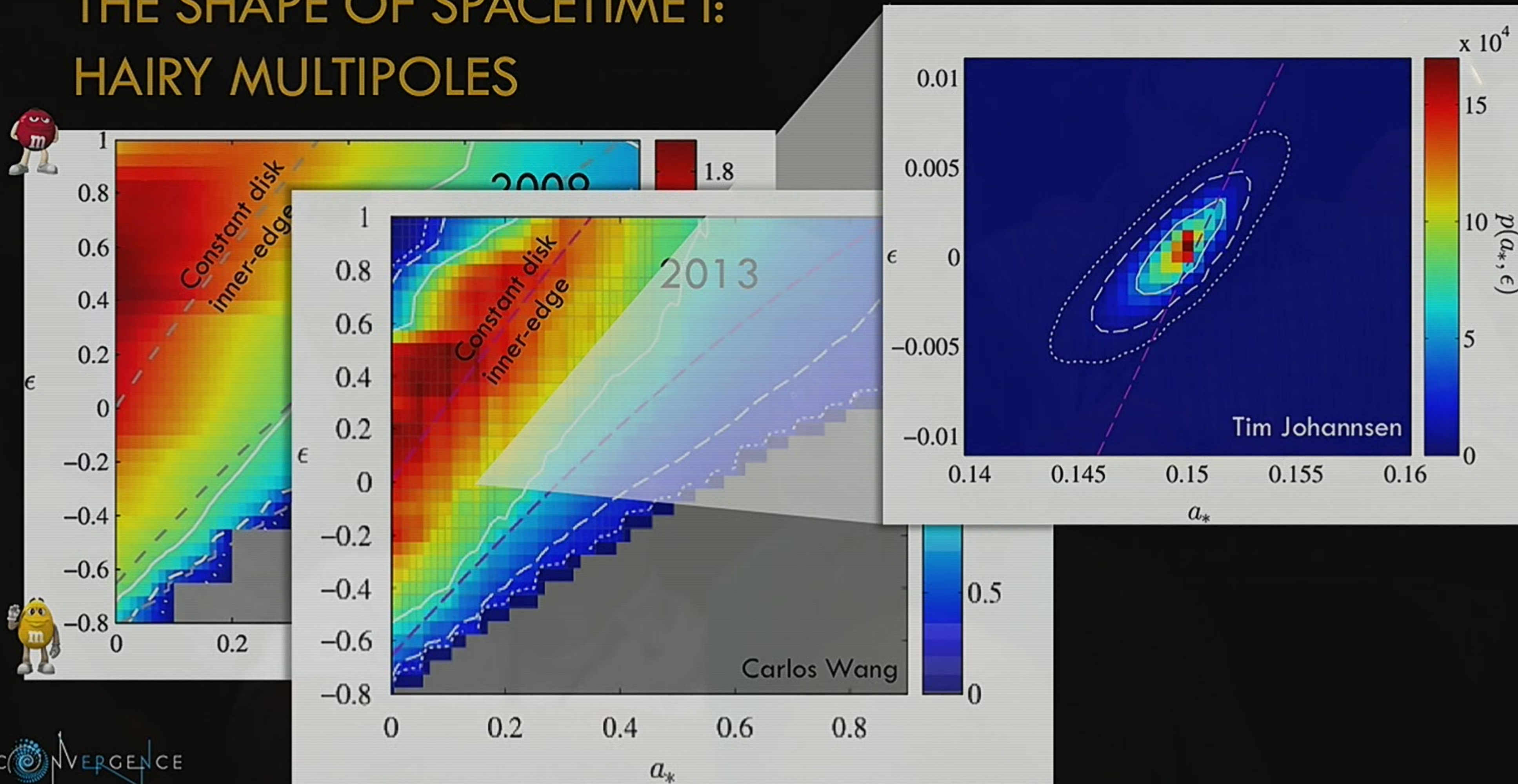

ONE OF THESE THINGS IS NOT LIKE THE OTHERS!

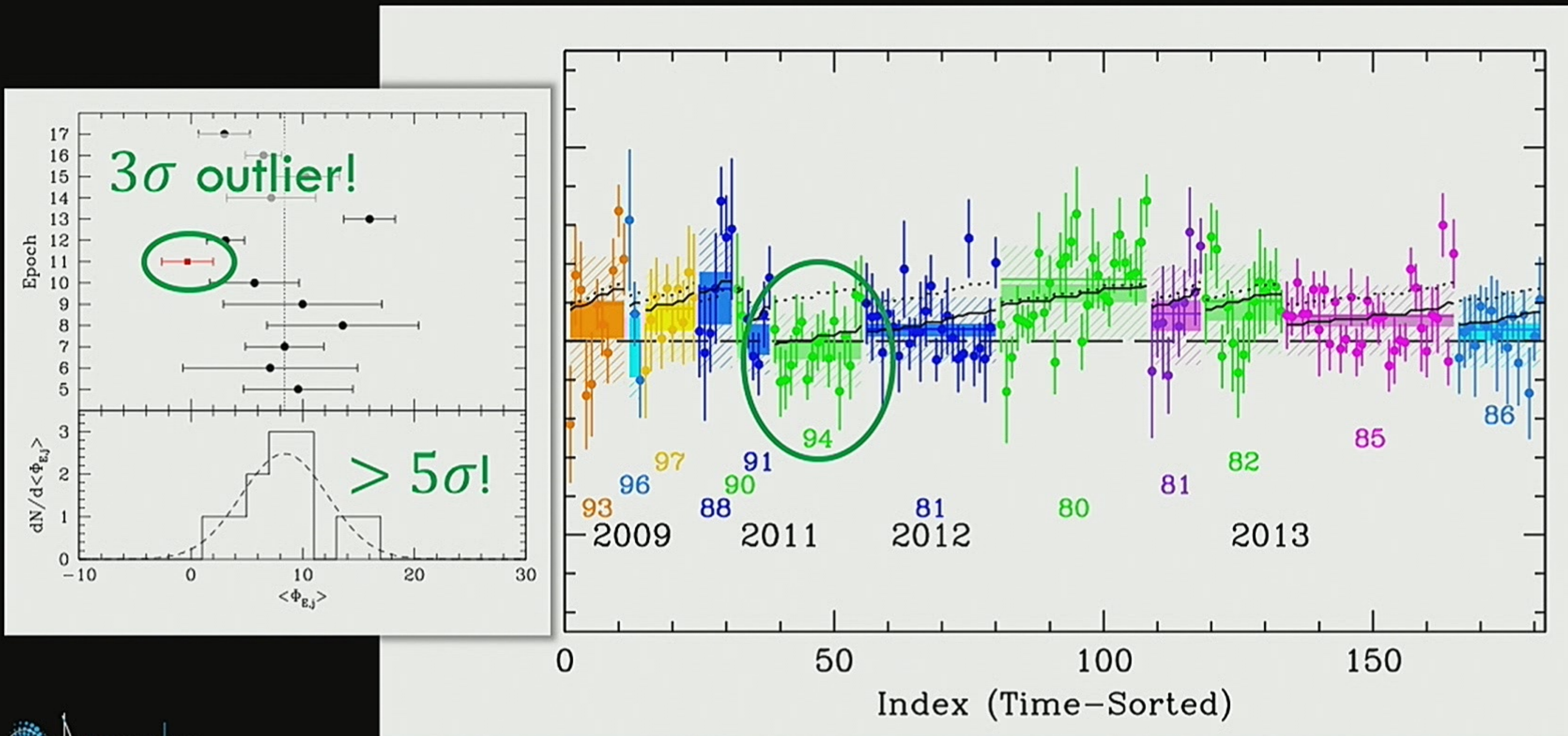


ONE OF THESE THINGS IS NOT LIKE THE OTHERS!
3σ outlier!
> 5σ!
Epoch
dN/d<Φ_E,j>
<Φ_E,j>
Infrared
Meyer et al. (2006)
X-ray
Baganoff et al. (2001)
Hard Band = 4.5–8 keV
Soft Band = 2–4.5 keV
HB cts/600 s
On Day 94 of 2011
224.1 GHz
Fish et al. (2015)
NRAO530-LL
SGRA-LL
Sgr A*
Calibrator
Amplitude
Time
2009
Keck/UCLA Galactic Center Group
CONVERGENCE

THE SHAPE OF SPACETIME II: SPACETIME TOMOGRAPHY

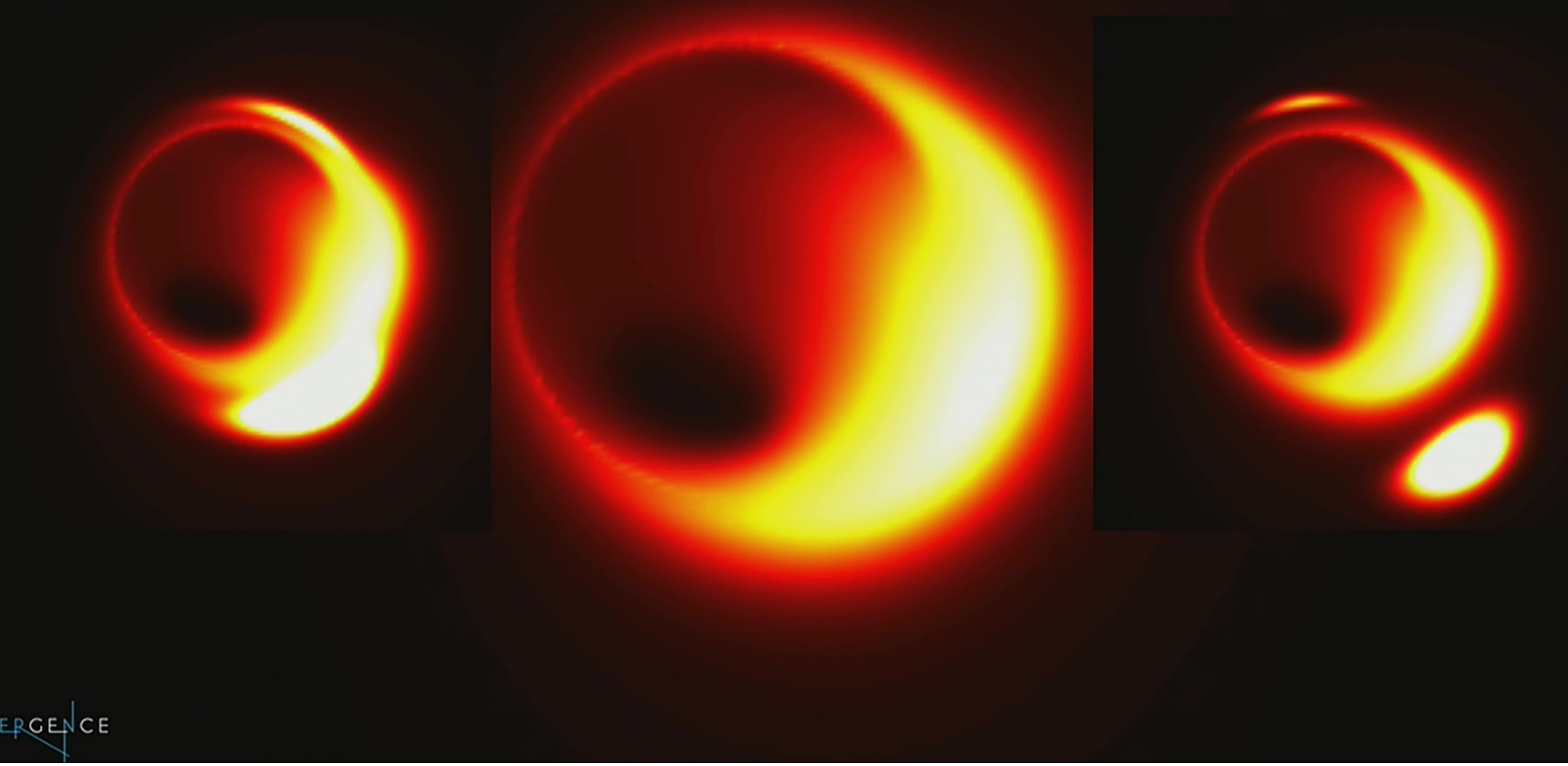

THE SHAPE OF SPACETIME II: SPACETIME TOMOGRAPHY

a = 0.9
Hot-spot at ~ 6M
Period = 27 min.

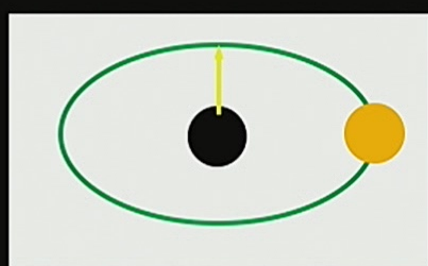

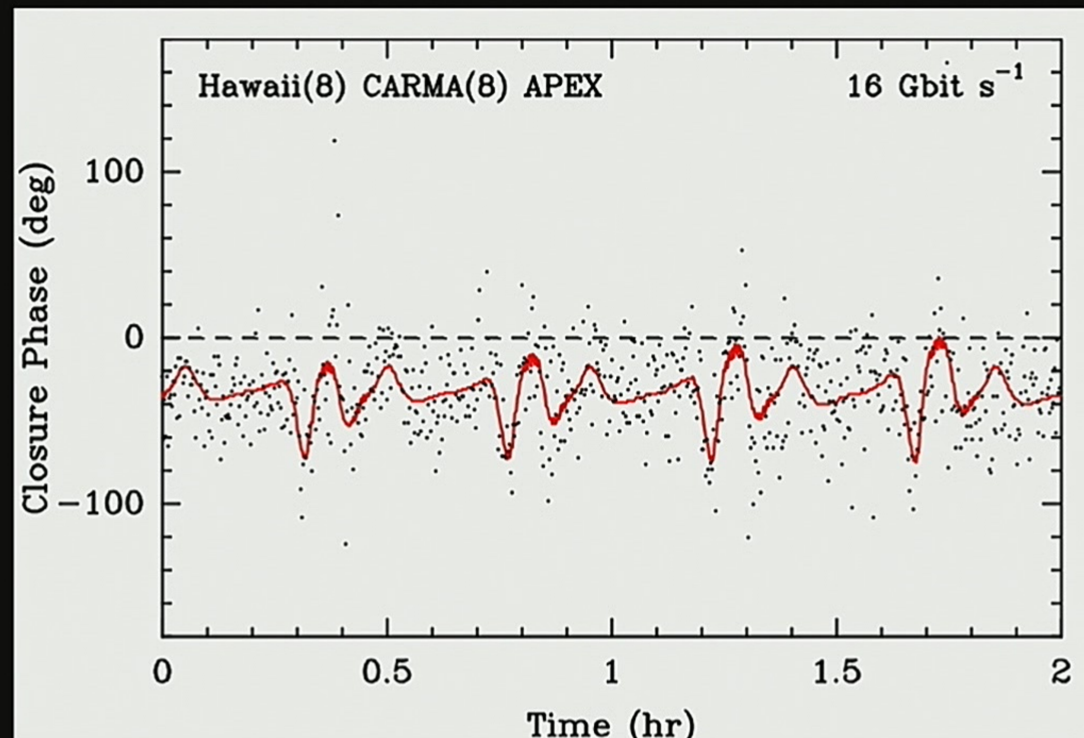

Doeleman, Fish, A.E.B., Loeb & Rogers (2009)

THE SHAPE OF SPACETIME III:
SPACETIME TOMOGRAPHY WITH POLARIZATION

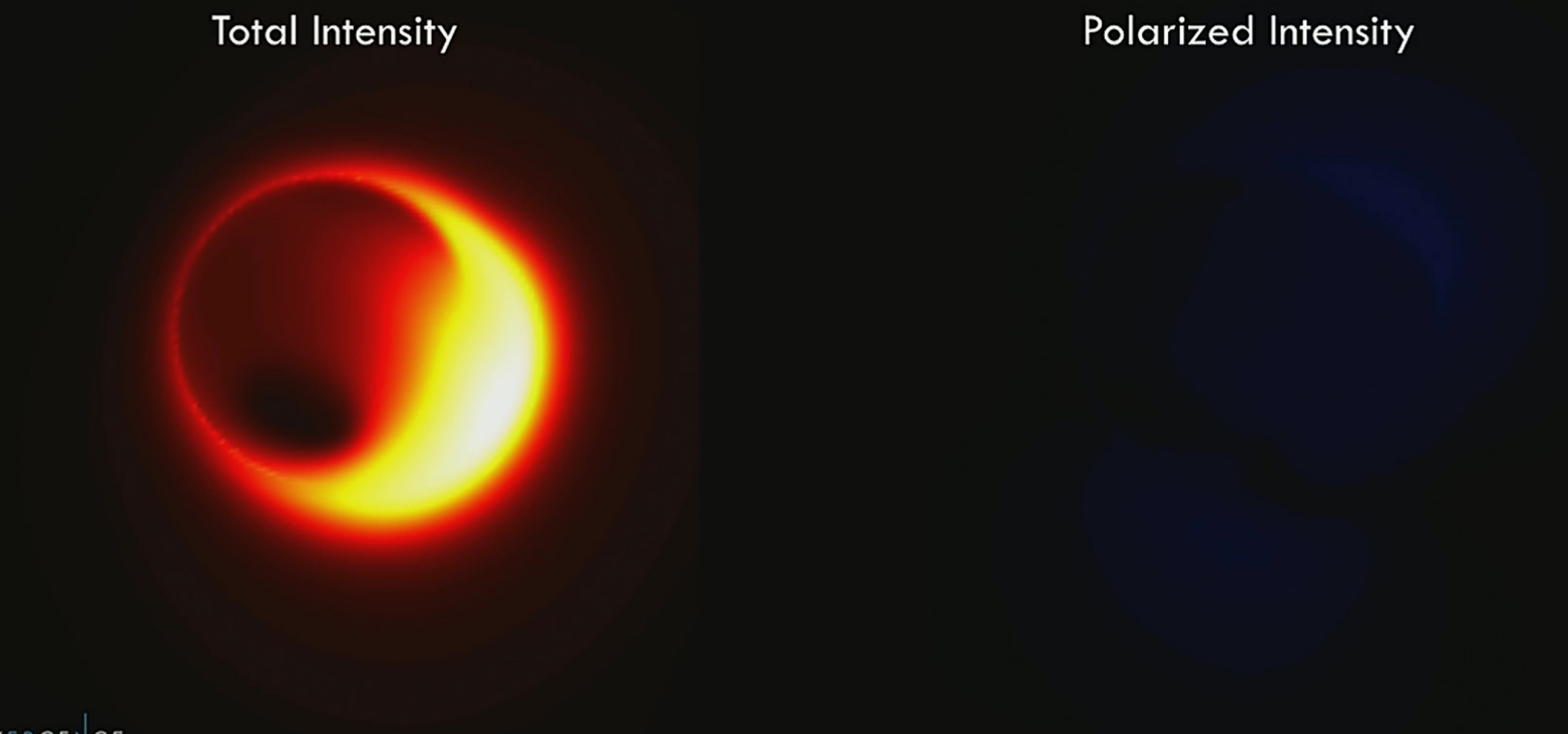

THE SHAPE OF SPACETIME III: SPACETIME TOMOGRAPHY WITH POLARIZATION

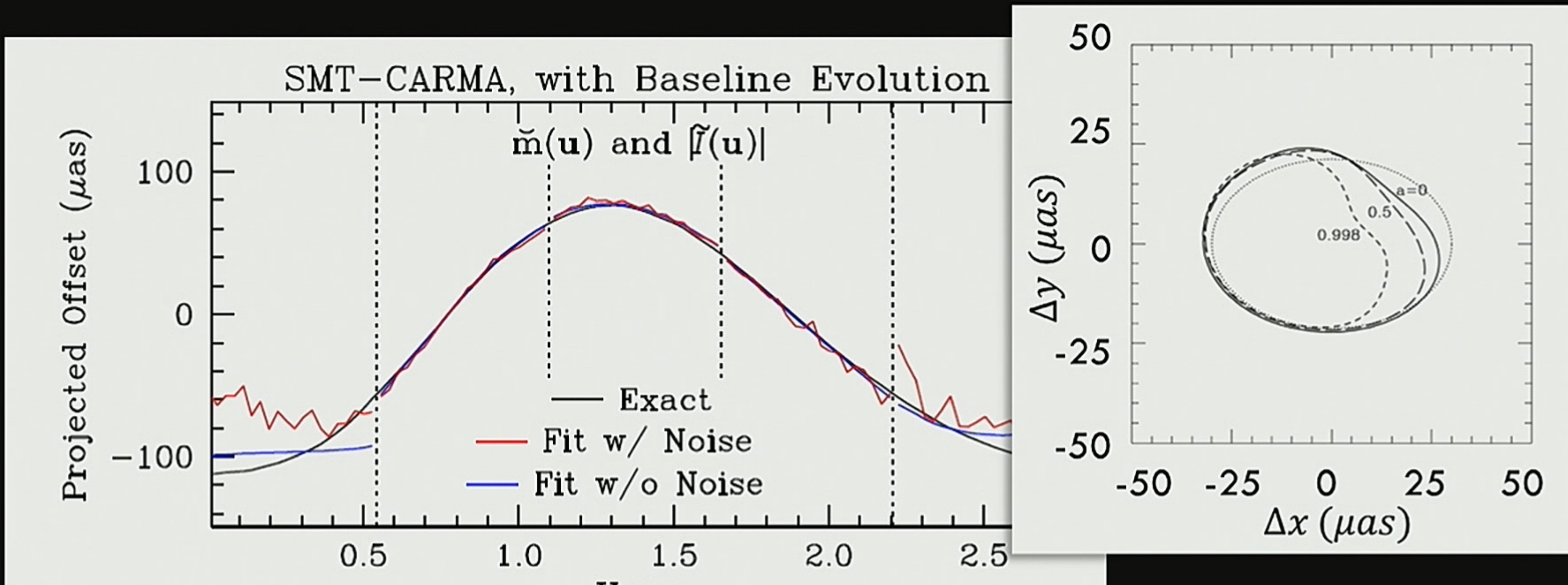

Johnson et al. (2014)